5-20-2011

A Practical Method for Power Systems Transient Stability and Security

Hussain Hassan Al Marhoon
University of New Orleans

A Practical Method for Power Systems Transient Stability and Security

A Thesis

Submitted to Graduate Faculty of the
University of New Orleans
in partial fulfillment of the
requirements for the degree of

Master of Science
in
Engineering
Electrical

By

Hussain Hassan Al Marhoon

B.S. University of New Orleans, 2008

May, 2010

To my parents and family

ACKNOWLEDGEMENT

This thesis would not have been possible without the guidance and help of several individuals who in one way or another contributed and extended their valuable assistance in the preparation and completion of this study.

First and foremost, I would like to express my utmost gratitude to my advisor, Professor Parviz Rastgoufard for his valuable guidance and selfless support during these two years of my Masters studies. His patience and unfailing encouragement have been the major contributing factors in the completion of my thesis research.

I am heartfelt thankful to my parents, sister and brothers for their never ending love and support.

Finally, I would like to thank all the professors and staff at the University of New Orleans who contributed in providing quality education. I would also like to thank the Saudi Ministry of Higher Education for supporting me financially throughout my studies.

TABLE OF CONTENTS

LIST OF TABLES viii

LIST OF FIGURES ix

ABSTRACT x

Chapter 1 1
INTRODUCTION 1
1.1 Overview 1
1.1.1 Power System Stability Problems 1
1.1.2 Forms of Power Instability 2
1.1.3 Classification of Stability 2
1.1.4 Why Power System Stability 4
1.2 Historical Review of Power System Stability Problems 4
1.3 Scope and Simulation Tools 7

Chapter 2 10
POWER SYSTEM STABILITY 10
2.1 Basic Concepts and Definitions 10
2.1.1 Rotor Angle Stability 11
2.1.2 Small-Signal Stability 16
2.1.3 Transient Stability 18
2.2 Review of Existing Methods of Transient Stability Analysis 19
2.2.1 Swing Equations 20
2.2.2 Equal-Area Criterion 21
2.2.3 Numerical Integration Methods 23
2.2.4 Direct Methods Transient Stability Analysis 24
2.3 Power System Models 25
2.3.1 Single-Machine Infinite-Bus 26
2.3.1.1 Classical Model 26
2.3.1.2 Detailed Model 27
2.3.2 Multi-Machine Infinite-Bus 29
2.3.2.1 Synchronous Reference Frame 29
2.3.2.2 Center of Inertia Reference Frame 30
2.4 Summary 31

Chapter 3 32
TRANSIENT STABILITY USING NUMERICAL METHODS 32
3.1 Overview 32
3.2 Numerical Integration Methods 32
3.2.1 Euler Method 32
3.2.2 Runge-Kutta Methods 33

3.2.2.1 Second-Order R-K Method ……...33
3.2.2.2 Forth-Order R-K Method ……..34
3.2.3 Implicit Integration Methods ……..... 35
3.3 Simulation of Power System Dynamic Response ……... 36
3.3.1 Overall System Equation …….. 36
3.3.2 Solution of Overall System Equation Using Implicit Integration Methods ……..37
3.4 Summary ……...38

Chapter 4 ……..... 40
TRANSIENT STABILITY USING DIRECT METHODS ……40
4.1 Overview ……... 40
4.2 Lyapunov's Method ……40
4.3 Transient Energy Function Formulation …….. 41
4.3.1 Main Idea …….. 41
4.3.2 Mathematical Development ……..42
4.3.3 Mathematical Development of TEF of Multi-machine Power Systems ……...43
4.3.3.1 Synchronous Reference Frame ……43
4.3.3.2 Center of Inertia Reference Frame …….....44
4.4 Multi-machine Transient Stability Measures Using TEF …… 46
4.4.1 Individual Machine Energy Function for Synchronous Reference Frame ……... 46
4.4.2 Individual Machine Energy Function for COI Reference Frame …… 48
4.4.3 Extended Equal Area Criterion ……50
4.4.4 Proposed Method …….. 53
4.5 Summary ……...54

Chapter 5 ……..... 56
TEST SYSTEM ……..56
5.1 IEEE 39 Bus Test System ……..... 56
5.1.1 Transmission Lines ……... 57
5.1.2 Transformers ……57
5.1.3 Generators ……58
5.1.4 Loads ……59
5.2 Summary ……...60

Chapter 6 ……..... 61
SIMULATION AND RESULTS …….. 61
6.1 Methodology ……61
6.1.1 Energy Comparison for Single Machine ……...61
6.1.2 Determining Critical Clearing Time ……62
6.2 Power System Analysis Toolbox (PSAT) in MATLAB ……..... 65
6.2.1 Overview ……...65
6.2.2 Models and Algorithms for Numerical Simulation …….. 67
6.2.2.1 Power System Model ……..... 67
6.2.2.2 Power Flow ……... 67
6.2.2.3 Time-Domain Simulation …… 68
6.3 Simulation Results ……... 68

6.3.1 Power Flow Results Using PSAT 68
6.3.2 Numerical Simulation in PSAT 68
6.3.3 Kron Reduction of Y-matrix 71
6.3.4 Determination of Severely Disturbed Groups 74
6.3.5 TEF for COI Reference Frame with Classical Model 75
6.3.6 TEF for Synchronous Reference Frame with Classical Model 81
6.4 Summary 83

Chapter 7 84
CONCLUDING REMARKS AND FUTURE WORK 84
7.1 Concluding Remarks 84
7.2 Future Work 86

Appendix A 87
A.1 Software Development 87
A.2 PSAT Built-in Functions 88
A.3 Power Flow Report 93

BIBLIOGRAPHY 98

VITA 101

LIST OF TABLES

5.1 Transmission Lines Data
5.2 Transformers Data
5.3 Generators' Initial Load Flow
5.4 Generators Details
5.5 Loads Data

6.1 SDG Determination Illustration
6.2 Total Energy Comparison
6.3 EEAC Method
6.4 Proposed Method Simulation for COI Reference Frame
6.5 Average Simulation Time
6.6 Determining Critical Clearing Time Using the Proposed Method
6.7 Comparison of the four methods in determining t_{cr}
6.8 Proposed Method Simulation for Synchronous Reference Frame
6.9 Average Simulation Time

A.2.1 Bus Data Format
A.2.2 Line Data Format
A.2.3 Transformer Data Format
A.2.4 Slack Generator Data Format
A.2.5 PV Generator Data Format
A.2.6 PQ Load Data Format
A.2.7 Fault Data Format
A.2.8 Synchronous Machine Data Format

LIST OF FIGURES

1.1 Classification of power system stability

2.1 Single line diagram and equivalent circuit of a two-machine system
2.2 Phasor diagram of power transfer characteristic of a two-machine system
2.3 Power-angle characteristic of a two-machine system
2.4 Nature of small-disturbance response with constant field-voltage
2.5 Nature of small-disturbance response with excitation control
2.6 Rotor angle response to a transient disturbance
2.7 Simple SMIB system
2.8 Power-angle characteristic of the system in Fig. 2.7
2.9 A ball rolling on the inner surface of a bowl
2.10 Single-machine infinite-bus system

3.1 Euler's method illustration

4.1 Potential energy plot
4.2 SMIB system

5.1 IEEE 39 Bus System

6.1 Flow chart of the proposed method applied to the IEEE 39 Bus system
6.2 Rotors' speeds and angles relative to COI using forward Euler's method plots
6.3 Rotors' speeds and angles relative to COI using Trapezoidal rule plots
6.4 Obtained plots of generator 2 rotor's angle and speed using forward Euler and Trapezoidal rule
6.5 Rotors' angles and speeds relative to synchronous reference frame plots using forward Euler

ABSTRACT

Stability analysis methods may be categorized by two major stability analysis methods: small-signal stability and transient stability analyses. Transient stability methods are further categorized into two major categories: numerical methods based on numerical integration, and direct methods.

The purpose of this thesis is to study and investigate transient stability analysis using a combination of step-by-step and direct methods using Equal Area Criterion. The proposed method is extended for transient stability analysis of multi machine power systems. The proposed method calculates the potential and kinetic energies for all machines in a power system and then compares the largest group of kinetic energies to the smallest groups of potential energies. A decision based on the comparison can be made to determine stability of the power system. The proposed method is used to simulate the IEEE 39 Bus system to verify its effectiveness by comparison to the results obtained by pure numerical methods.

Key Words: Transient stability, direct methods, numerical methods, Equal Area Criterion, energy function, critical machine

CHAPTER 1

INTRODUCTION

1.1 Overview:

Power systems generally consist of three stages: generation, transmission, and distribution. In the first stage, generation, the electric power is generated mostly by using synchronous generators. Then the voltage level is raised by transformers before the power is transmitted in order to reduce the line currents which consequently reduce the power transmission losses. After the transmission, the voltage is stepped down using transformers in order to be distributed accordingly.

Power systems are designed to provide continuous power supply that maintains voltage stability. However, due to undesired events, such as lightning, accidents or any other unpredictable events, short circuits between the phase wires of the transmission lines or between a phase wire and the ground which may occur is called a *fault*. Due to occurring of a fault, one or more generators may be severely disturbed causing an imbalance between generation and demand. If the fault persists and is not cleared in a pre-specified time frame, it may cause severe damages to the equipments which in turn may lead to a power loss and power outage. Therefore, protective equipments are installed to detect faults and clear/isolate faulted parts of the power system as quickly as possible before the fault energy is propagated to the rest of the system.

1.1.1 Power System Stability Problem:

Power system stability is a very important aspect to supply continuous power. It is defined as that property of a power system that enables it to remain in a state of operating

equilibrium under normal operating conditions and to regain an acceptable state of equilibrium after being subjected to a disturbance [1]. Instability of power system can occur in many different situations depending on the system configuration and operating mode. One of the stability problems is maintaining synchronous operation or synchronism especially that power system rely on synchronous machines. This aspect is influenced by the dynamic of generator rotor angles and power-angle relationships. Other instability problem that may be encountered is voltage collapse that is mostly related to load behavior and not synchronous speed of generators.

1.1.2 Forms of Power Instability:

There are three different forms of power system instability: rotor angle instability, voltage instability and voltage collapse, and mid-term and long-term instability. *Rotor angle stability* is the ability of interconnected synchronous machines of a power system to remain in synchronism. *Voltage stability* is the ability of a power system to maintain acceptable voltages at all buses in the system under normal operating conditions and after being subjected to a disturbance. For the voltage to be stable, the synchronous machines must run in synchronism. The *long-term* and *mid-term stability* are relatively new to the literature on power system stability [1]. Long-term stability is associated with the slower and longer-duration phenomena that accompany large-scale system upsets and on the resulting large, and sustained mismatches between generation and consumption of active and reactive power. In mid-term stability, the focus is on synchronizing power oscillations between machines, including the effects of some of the slower phenomena and possibly large voltage or frequency excursions [1].

1.1.3 Classification of Stability:

Figure 1.1 [1] provides a comprehensive categorization of power system stability. As depicted by Figure 1.1, there are two main classes of stability: *angle stability and voltage*

stability. Angle stability has two main subclasses: *small-signal (steady-state) stability* and *transient stability*. A power system is considered to be *steady-state stable* if, after any small disturbance, it reaches a steady state operating condition which is identical or close to the pre-disturbance operating condition. A power system is transient stable for a large disturbance or sequence of disturbances if, following that disturbance(s) it reaches an acceptable steady-state operating condition. Unlike steady-state stability which is a function only of the operating condition, transient stability is more complicated since it is a function of both operating condition and the disturbance [2]. Voltage stability also has two main subclasses: *large-disturbance voltage stability and small-disturbance voltage stability*.

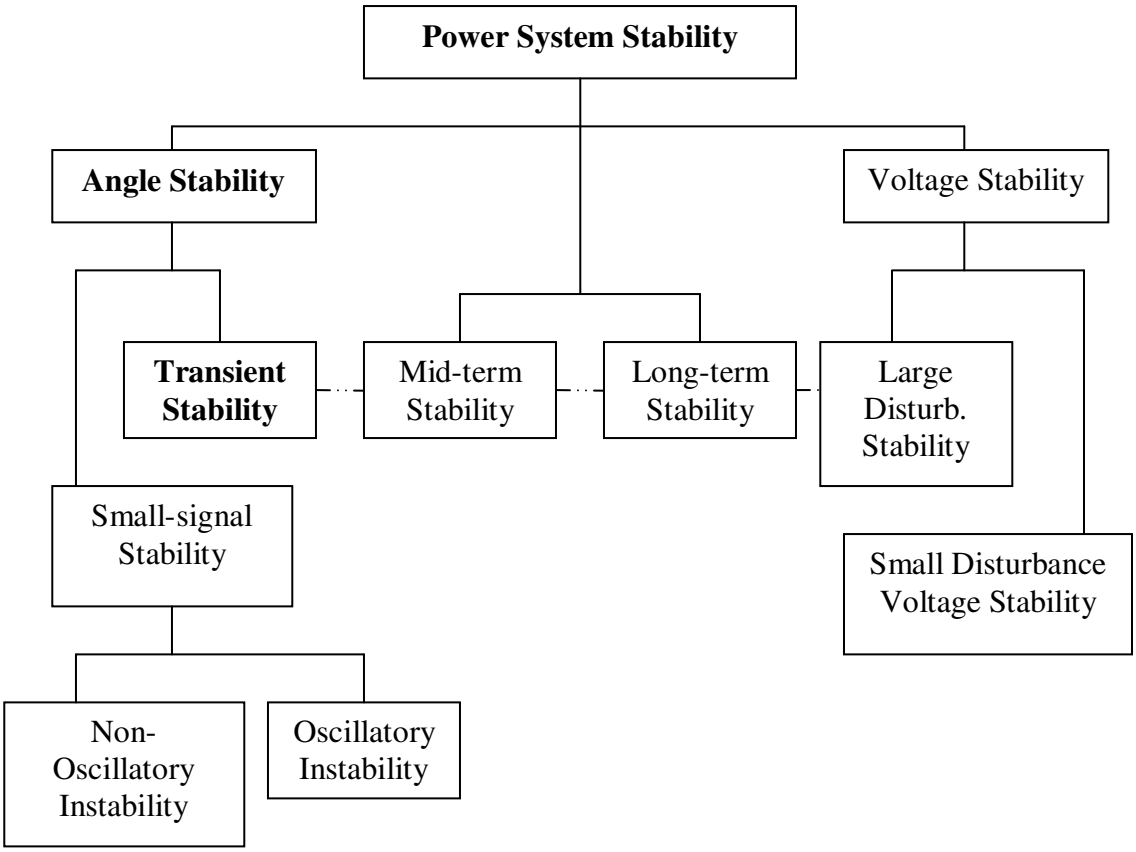

Figure 1.1: Classification of power system stability [1]

For transient stability, it is usually when the power system experiences a large disturbance caused by an imbalance between the mechanical input and the electrical output powers. In order to study this type of stability, the focus is only on the first swing periodic drift. Therefore, only a fraction of a second is enough to observe the transients and several simulation time seconds to study the system. As of the small-signal stability, it occurs when the system lacks synchronizing torque or when an unstable control action occurs. This type of stability requires a study of more than a minute to several hours.

1.1.4 Why Power System Stability:

Power system stability is a complex subject that has challenged power system engineers for many years. Power systems operate closer and closer to their limits which makes the instability problem to be more probable. With that given, it is very important to detect any disturbance that may cause the instability. Instability may occur during steady-state; however, it occurs more frequently following short-circuits which makes the time to clear a large disturbance to be very short. That is, it is very crucial to determine whether the system will be transient stable or will lose its synchronism. Therefore, transient stability analysis requires very fast computation and decision making.

1.2 Historical Review of Power System Stability Problems:

Different forms of instability have emerged over the last century. The methods of power system stability problems analysis were influenced by the development of computational tools, stability theories, and power system control technologies. Therefore, it is very essential to present a review of the history of the subject to better understand the methods used in industries with regard of system stability and how these developments relate to the proposed practical method in the thesis.

Power system stability is a complex problem that has challenged power system engineers for many years. It was first recognized as an important problem in 1920s (Steinmetz, 1920; Evans and Bergvall, 1924; Wilkins 1926) [3]. The first field tests on the stability on a practical power system were conducted in 1925 [4, 5]. The early stability problems were associated with remote power plants feeding load centers over long transmission lines. With slow exciters and non-continuously acting voltage regulators, power transfer capability was often limited by steady-state as well as transient rotor angle instability due to insufficient synchronizing torque [6].

In the early years, graphical methods such as, Equal Area Criterion (EAC) and power circle diagrams were developed. These methods were successfully applied to early systems that could be represented as two-machine systems. As the systems become larger, and interconnection which was found to be economically better, the complexity of the systems grew and therefore the stability problems became more complex, which voided the treatment of the systems to be two-machine systems. A significant step towards the improvement of stability calculations was the development in 1930 of the network analyzer which was capable of power flow analysis of multi-machine power systems [1, 6]. A network analyzer is essentially a scaled model of an AC power system with adjustable resistors, inductors and capacitors to represent the transmission network and loads, voltage sources whose magnitude and angle are adjustable, and meters to measure voltages, currents, and power anywhere in the network. However, system dynamic still had to be solved by hand by solving the swing equations using step-by-step numerical integration. During this period, classical models were used for the swing equations; that is, by representing the generators by fixed transient reactances and a fixed power supply behind these reactances.

In the early 1950s, electronic analog computers were used for analysis of special problems requiring detailed modeling of the synchronous machine, excitation system, and speed governor. Also, during that period, development of digital computers was seen, and specifically about 1956, the first digital program for power system stability analysis was developed. In the 1960s, most of the power systems in the United States and Canada were joined as part of one of two large interconnected systems, one in the east and the other in the west. In 1967, low capacity HVDC ties were also established between the east and west systems. Nowadays, the power systems in the United States and Canada form virtually one large system. This interconnection between the two systems result in operating economy and increased reliability, though, it increased the complexity of stability problems and increase the consequences of instability [1].

Until recently, most industry effort and interest has been concentrated on transient (rotor angle) stability [1]. Powerful transient stability simulation programs have been developed that are capable of modeling large complex systems using detailed models. In the early 1990s, the focus was on small-signal stability which then led to the development of special study techniques, such as modal analysis using eigenvalue techniques.

In the 1970s and 1980s, frequency stability problems were experienced following major system upsets led to an investigation of the underlying causes of such problems and to the development of long-term dynamic simulation programs to assist in their analysis. In 1983, guidelines were developed for enhancing power plant response during major frequency disturbance.

Nowadays, power systems are being operated under increasingly stressed condition due to the prevailing trend to make the most of existing facilities. Increased competition, open transmission access, and construction and environmental constraints are shaping the operation of

electric power systems which present greater challenges for secure system operation. This is clear from the increasing number of major power-grid blackouts that have been experienced in recent years such as, Northeast USA-Canada blackout of August 14, 2003. Planning and operation of today's power systems require a careful consideration of all forms of system instability. Significant advances have been made in recent years in providing better tools and techniques to analyze instability in power systems.

1.3 Scope and Simulation Tools:

It is very important for electric utilities to provide continuous power supply with minimal interruption. In order to do that, it is essential to install protecting equipments such as, circuit breakers and protective relays which protect the synchronous generators and transmission lines. The purpose of this thesis is to find new ways to help in transient stability assessment for multi-machine power systems during planning and operation (on-line assessment) phases. For this purpose, direct methods are the most appropriate and the fastest methods to determine stability of power systems. However, due to the complication of these methods when applied to larger systems, variety of direct methods will be tested. Essentially, these methods are all based on *transient energy function* (TEF) phenomena.

In this thesis, we propose a faster way to apply *extended equal area criterion*. The proposed method requires three points: the *stable equilibrium point* (SEP) which is known from the steady-state setup, rotor angles at the clearing time, and the estimate of *unstable equilibrium points* (UEP). In traditional direct methods, the UEP is estimated by using only simulation results up to the clearing time. However, in our proposed, we continue using simulation up to critical clearing time, a longer simulation time than clearing time but much smaller than the simulation time that is used in step-by-step integration of the model. The method is based on simulating the

system from the moment of a fault occurrence until the critical clearing of that fault using numerical methods. Then, the results of the numerical integration are used to: first, determine the unstable equilibrium points, then, calculate the potential and kinetic energies for each generator on the system, and finally, determine whether the system is stable or unstable. When the potential energy of each individual machine is found, the potential energies are sorted in ascending order. Similarly, when the kinetic energy of each individual machine is found, the kinetic energies are sorted in descending order. After calculating the potential and kinetic energies of each machine in the system, the system is separated into two groups: the severely disturbed group of machines, and the less disturbed machines. The severely disturbed group of machines is determined using the accelerating power. Then, the group of the largest kinetic energy is compared to the same number of group of smallest potential energy. If the largest kinetic energy is smaller than the smallest potential energy, then the system is stable; otherwise, the system is unstable. It is very challenging to find the *unstable equilibrium point* using the post-fault system settings, but since the purpose of this thesis is stability assessment using energy functions, previous methods will be implemented to calculate the UEP.

Additionally, this thesis provides comparison between the different direct methods with the numerical methods and the proposed method results. In the comparison, simulation time is captured for each method and the accuracy is compared with the numerical methods as a benchmark.

The proposed method and the previous methods will be simulated and tested on the IEEE 39 Bus (New England) equivalent power system. This system has a total of 39 Buses of which 10 Buses are generator buses. The data of this system will be provided in Chapter 5.

MATLAB is a numerical computing environment that can be used for transient stability analysis using the *Power System Analysis Toolbox* (PSAT.) PSAT is a MATLAB toolbox for static and dynamic analysis and control of electric power systems [10]. PSAT includes all the required tools such as, power flow and time domain simulation, to simulate and analyze the methods in this thesis.

In this thesis, first, a general discussion of power system stability and review of previous methods are provided in chapter 2. Also, the general models of multi-machine power systems are introduced in chapter 2. Then, in chapter 3, transient stability analysis using numerical methods is discussed in detail. In chapter 4, transient energy function is introduced and different direct methods in transient stability analysis are provided with their mathematical formulations and criterion used to determine stability. Also, the proposed method is introduced and discussed in chapter 4. In chapter 5, the IEEE 39 Bus power system is presented and its parameters are tabulated. In chapter 6, some of the direct methods explained in chapter 4 are simulated on the IEEE 39 Bus system and these methods are compared with the proposed method and the numerical integration, which is used as a benchmark. Finally, some concluding remarks and future work are presented in chapter 7. In the appendices, software developments of the functions used in this thesis are briefly presented. In addition, the formatting of the various PSAT built-in functions and scripts are briefly explained.

CHAPTER 2

POWER SYSTEM STABILITY

2.1 Basic Concepts and Definitions

Power system stability may be defined as that property of a power system that enables it to remain in a state of operating equilibrium under normal operating conditions and to regain an acceptable state of equilibrium after being subjected to a disturbance [1].

Instability of power system can occur in many different situations depending on the system configuration and operating mode. Traditionally, the stability problem has been to maintain synchronous operation or synchronism especially since power systems generation relies on operation of synchronous machines. Necessary condition for satisfactory system operation is that all synchronous machines operate in synchronism. This aspect is influenced by the dynamics of the generator rotor angles and power-angle relationship.

In the stability assessment, the concern is the behavior of the power system when subjected to transient disturbance. The disturbance may be small in the form of load changing conditions, or large in the form of short-circuit on a transmission line or other large disturbances such as, loss of large load or generator, or loss of tie-line between two subsystems. The system response to a disturbance involves much of the equipment. For example, a short-circuit on a critical element followed by its isolation by protective relays will cause variations in power transfers, machine rotor speeds, and bus voltages; the voltage variations will actuate both generator and transmission system voltage regulators; the speed variation will actuate prime mover governors; the change in tie line loading may actuate generation controls; the changes in

voltage and frequency will affect loads on the system in varying degrees depending on their individual characteristics [1]. Many assumptions are usually made to simplify the problem and to focus on factors influencing the specific type of stability problem.

To provide a framework for our proposed method, we briefly describe different form of power system instability and associated concepts. Analysis of small idealized system will be used to show each type of instability.

2.1.1 Rotor Angle Stability

Rotor angle stability is the ability of interconnected synchronous machines of a power system to remain in synchronism [1]. The stability problem involves the study of the electromechanical oscillations inherent in power systems. A fundamental factor in this problem is how the outputs of synchronous machines vary with respect to their rotors oscillations. A brief discussion of synchronous machines characteristics is helpful to develop the basic concepts of stability.

A synchronous machine has two essential circuits: the field, which is on the rotor, and the armature, which is on the stator. The field winding is supplied by direct current power while the terminals of the armature provide the load power. The rotating magnetic field of the field winding induces alternating voltages when the rotor is driven by a prime mover (turbine). The frequency of the induced voltages depends on the speed of the rotor and the number of poles of the machine. The frequency of the electrical voltage and the rotor mechanical speed are synchronized (or in synchronism), at *60 Hz* in USA, Canada and South America, and *50 Hz* in most other countries.

When two or more synchronous machines are interconnected, the stator voltages and currents must have the same frequency and the rotor mechanical speed of each machine is synchronized to this frequency.

To change the electrical torque (or power) output of the generator, the mechanical torque input is changed to advance the rotor to a new position relative to the revolving magnetic field of the stator.

Consider the system shown in Figure 2.1. It consists of two synchronous machines connected by a transmission line having an inductive reactance X_L but negligible resistance and capacitance. Assume that machine 1 represents a generator feeding power to a synchronous motor represented by machine 2.

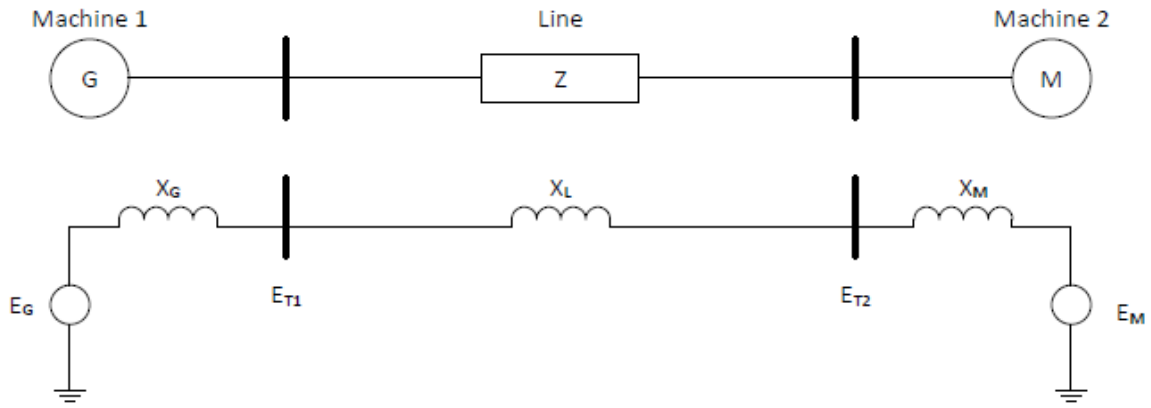

Figure 2.1: Single line diagram and equivalent circuit of a two-machine system [1]

The power transfer from the generator to the motor is a function of the angular separation δ between the rotors of the two machines. This angular separation is due to three components: generator internal angle δ_G, angular difference between the terminal voltages of the generator and motor, and the internal angle of the motor.

A phasor diagram identifying the relationships between generator and motor voltages is shown in Figure 2.2. The power transferred from the generator with reactance of X_G to the motor with reactance of X_M through a transmission line with reactance of X_L is given by Equation 2.1.

$$P = \frac{E_G E_M}{X_T} \sin \delta \tag{2.1}$$

where

$$X_T = X_G + X_L + X_M$$

The corresponding power versus angle relationship is plotted in Figure 2.3. In the equivalent model, an idealized model is used which makes the power varies as a sine of the angle. However, with a more accurate machine models including the effects of automatic voltage regulators, the variation in power with angle would deviate significantly from the sinusoidal relationship, but the general form would be similar. As the angle is increased, the power transfer increases up to a maximum. After a certain angle, normally 90˚, a further increase in angle results in a decrease in power. When the angle is zero, no power is transferred.

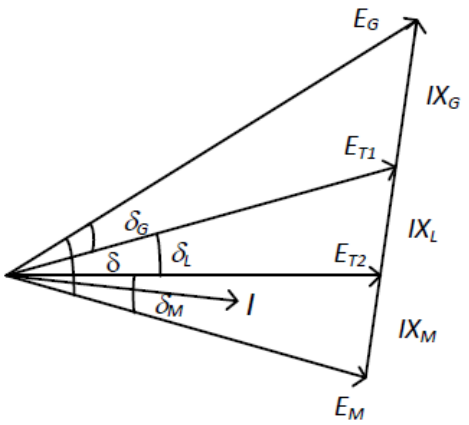

Figure 2.2: Phasor diagram or power transfer characteristic of a two-machine system [1]

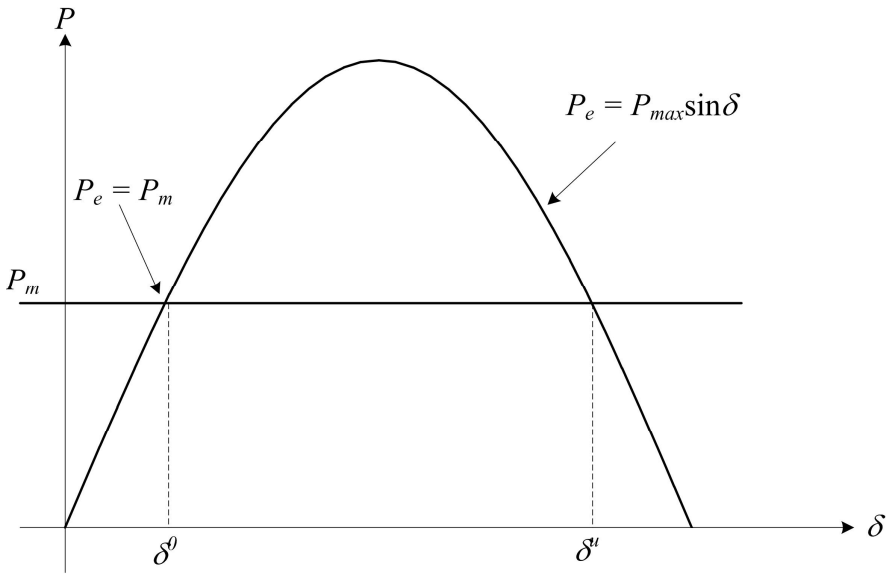

Figure 2.3: Power-angle characteristic of a two-machine system [1]

From Figure 2.3, there are two points of interest: stable equilibrium point δ^0 (SEP), and the unstable equilibrium point δ^u (UEP). In the steady-state status, the system rests on the SEP where the mechanical power is equal to the electrical power. However, if the system *swings* to the UEP, where the mechanical power is equal to the electrical power graphically, the synchronous machine loses synchronism (unstable). Note that the system is assumed to be lossless.

When there are more than two machines, their relative angular displacements affect the interchange of power in a similar manner. However, limiting values of power transfers and angular separation are a complex function of generation and load distribution.

Stability is a condition of equilibrium between opposing forces. The mechanism by which interconnected synchronous machines maintain synchronism with one another is through restoring forces, which act whenever there are forces tending to accelerate or decelerate one or more machine with respect to other machines. In steady-state, there is equilibrium between the input mechanical torque and the output electrical power of each machine, and the speed remains

constant. However, if the system is perturbed, this equilibrium is disturbed resulting in acceleration or deceleration of the rotors of the machines according to the laws of motion of a rotating body [1]. If one generator runs faster than the other, the rotor angle of the faster machine relative to the rotor angles of the slower machines will change and that particular machine may lose synchronism causing disturbance to the other machines. As previously discussed, beyond a certain limit, an increase in angular separation is accompanied by a decrease in power transfer; this increases the separation further which leads to instability. For any given situation, the stability of the system depends on whether or not the deviations in angular positions of the rotors result in sufficient restoring torque.

Loss of synchronism can occur between one machine and the rest of the system or between groups of machines. In this case, synchronism may be maintained within each group after its separation from the others.

The change in electrical torque of a synchronous machine following a perturbation can be resolved into two components:

$$\Delta T_e = T_s \Delta\delta + T_D \Delta\omega \qquad (2.2)$$

Where in Equation 2.2

$T_s \Delta\delta$ is the component of torque change in phase with the rotor angle perturbation $\Delta\delta$ and is referred to as *synchronizing torque* component; T_s is the synchronizing torque coefficient.

$T_D \Delta\omega$ is the component of torque change in phase with the speed deviation $\Delta\omega$ and is referred to as the *damping torque* component; T_D is the damping torque coefficient.

Lack of sufficient synchronizing torque may result in instability through an *aperiodic drift* in rotor angle. On the contrary, lack of sufficient damping torque results in *oscillatory instability*.

Rotor angle stability phenomenon is categorized into two main categories: *small-signal stability*, and *transient stability*.

2.1.2 Small-Signal Stability:

It is the ability of the power system to maintain synchronism under small disturbances. These types of disturbances occur on the system because of small variation in loads and generation. Instability that may result can be of two forms: (i) steady increase in rotor angle due to lack of sufficient synchronizing torque, or (ii) rotor oscillations of increasing amplitude due to lack of sufficient damping torque. The system response to small disturbance depends on: initial operation, the transmission system strength, and the type of generator excitation controls used. For a generator connected radially to a large power system, in the absence of automatic voltage regulators (i.e. with constant field voltage) the instability is due to lack of sufficient synchronizing torque. This result is shown in Figure 2.4. With continuously acting voltage regulators, the small-signal stability is one of ensuring enough damping of system oscillations. Figure 2.5 shows this type of instability.

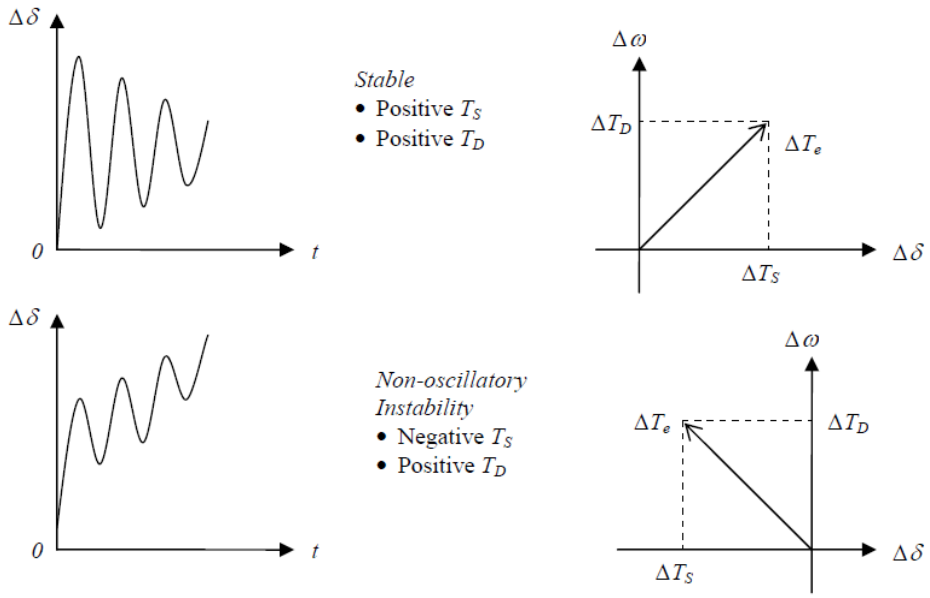

Figure 2.4: Nature of small-disturbance response with constant field voltage. Redrawn from [1]

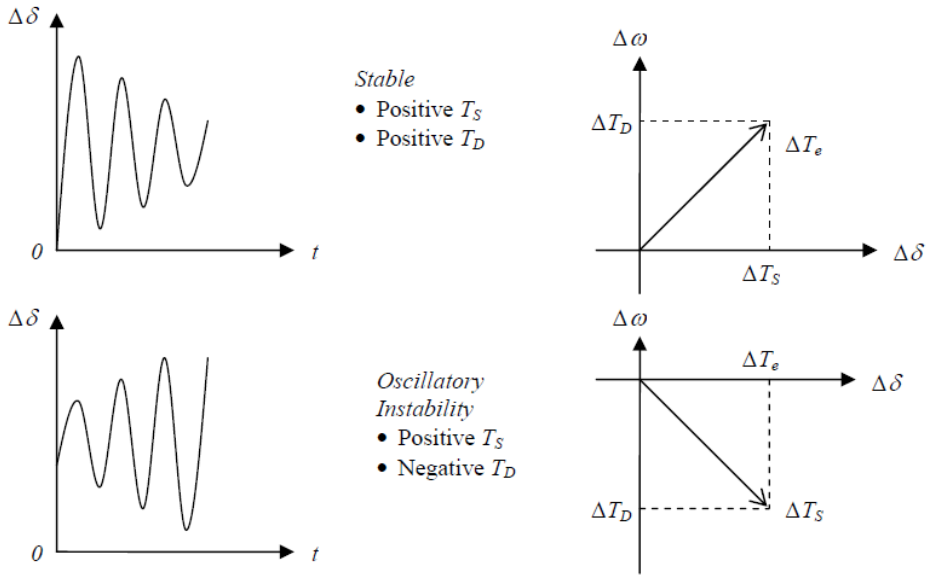

Figure 2.5: Nature of small-disturbance response with excitation control. Redrawn from [1]

Nowadays, practical power system may experience small-signal instability due to insufficient damping of oscillations. The stability of the following types of oscillations is of concern:

- *Local modes or machine-system modes*: these are associated with the swinging of units at a generating station with respect to the rest of the power system.

- *Interarea modes*: these are associated with the swinging of many machines in one part of the system against machines in other parts.
- *Control modes*: these are associated with generating units and other controls.
- *Torsional modes*: these are associated with the turbine-governor shaft system rotational components.

2.1.3 Transient Stability:

Transient stability is the ability of the power system to maintain synchronism when subjected to sever transient disturbance. The response to this type of disturbance involves large excursions of rotor angles and is influenced by nonlinear power-angle relationship. Stability depends on the initial operating state of the system and the severity of the disturbance. The system usually altered after the disturbance which may cause the system to operate in a different steady-state status from that prior the disturbance.

Power systems are designed to be stable for a selected set of contingencies. The contingencies usually considered are short-circuits of different types: phase-to-ground, phase-to-phase-to-ground, or three-phase. They are usually assumed to occur on the transmission lines, but occasionally bus or transformer faults are also considered.

Figure 2.6 illustrates the behavior of a synchronous machine for stable and unstable situations. In Case 1, the rotor angle increases to a maximum, then decreases and oscillates with decreasing amplitude until it reaches a steady state. This case is considered transient stable. In Case 2, the rotor angle continues to increase steadily until synchronism is lost. This type on transient instability is referred to as *first-swing* instability. In Case 3, the system is stable in the first swing but becomes unstable as a result of growing oscillations as the end state is

approached. This form of instability occurs when the postfault steady-state condition is itself is small-signal unstable.

In transient stability studies, the study period of interest is usually limited to 3 to 5 seconds following the disturbance, although it may extend to about ten seconds for very large systems with dominant interarea modes of oscillation.

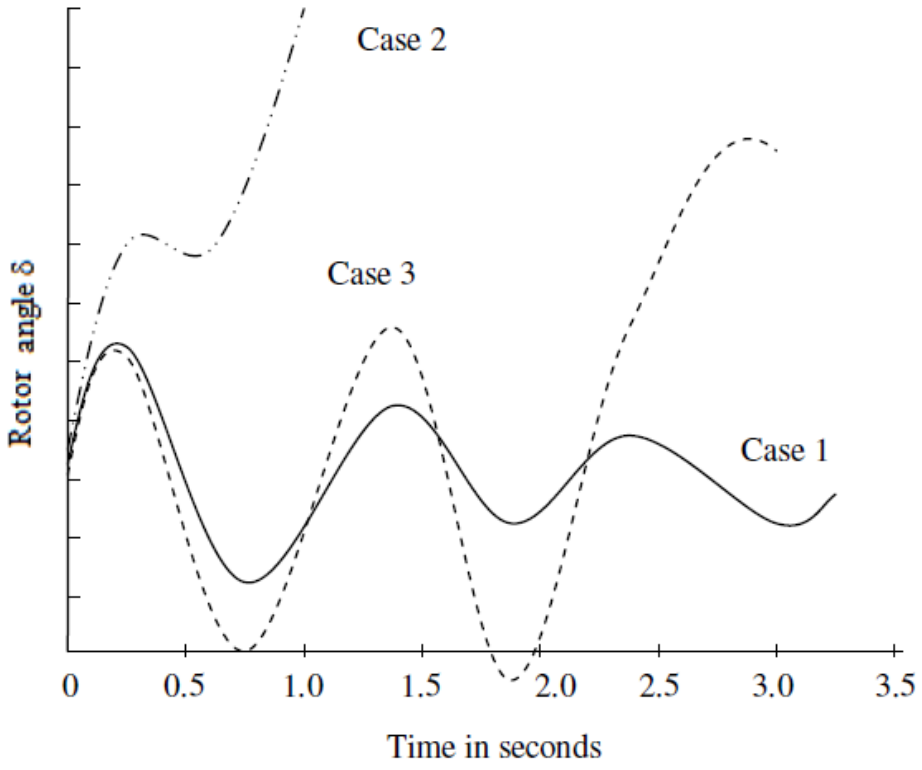

Figure 2.6: Rotor angle response to a transient disturbance. Redrawn from [1]

2.2 Review of Existing Methods of Transient Stability Analysis:

As previously explained, transient stability is the ability of the power system to maintain synchronism when subjected to a severe transient disturbance such as a fault on transmission facilities, loss of generation, or loss of a large load. The system response to such disturbances involves large excursions of generator rotor angles, power flows, bus voltages, and other system variables. If the resulting angular separation between the machines in the system remains within

certain bounds, the system maintains synchronism. If loss of synchronism occurs, the transient instability will be evident within 2 to 3 seconds of the occurrence of the disturbance.

In this section, different methods of transient stability analysis are briefly introduced. Since the focus of this thesis is transient stability analysis, small-signal stability analysis is not explained in this section. Also, before introducing some of the methods, it is essential to introduce the swing equation to represent the dynamic of a power system.

2.2.1 Swing Equation:

The swing equation describes the rotational dynamics of a synchronous machine and is used in stability analysis to characterize that dynamic. During normal operation, the relative position of the rotor axis and the resultant axis is fixed. During disturbance to the machine, the rotor either accelerates or decelerates with respect to the synchronous rotating air gap MMF [7]. The swing equation describes this relation.

The swing equation of a power system is given as:

$$M\ddot{\delta} + D\dot{\delta} + P_G(\delta) = P_M^0 \tag{2.3}$$

Where $M \triangleq H / \pi f_0$

H is the per unit inertial constant, $H \triangleq \dfrac{W_{kinetic}^{0}}{S_B^{3\phi}} = \dfrac{\text{kinetic energy}}{\text{3-phase apparent power}}$

$D \triangleq 2k\omega_0 / S_B^{3\phi}$

$P_G(\delta)$ is the electrical power in p.u

P_M^0 is the per unit mechanical power

δ is the relative angle of the electrical power

k is damping constant

ω_0 is the base electrical frequency in rad/sec

With the swing equation idea introduced, transient stability can be introduced in the following sections.

2.2.2 Equal-Area Criterion

Consider a single-machine infinite-bus (SMIB) system of Figure 2.7. For the system model considered in Figure 2.7, it is not necessary to formally solve the swing equation to determine whether the rotor angle increases indefinitely or oscillates about an equilibrium position. Assume that the system is a purely reactive, a constant P_m and constant voltage behind transient reactance for the system in Figure 2.7.

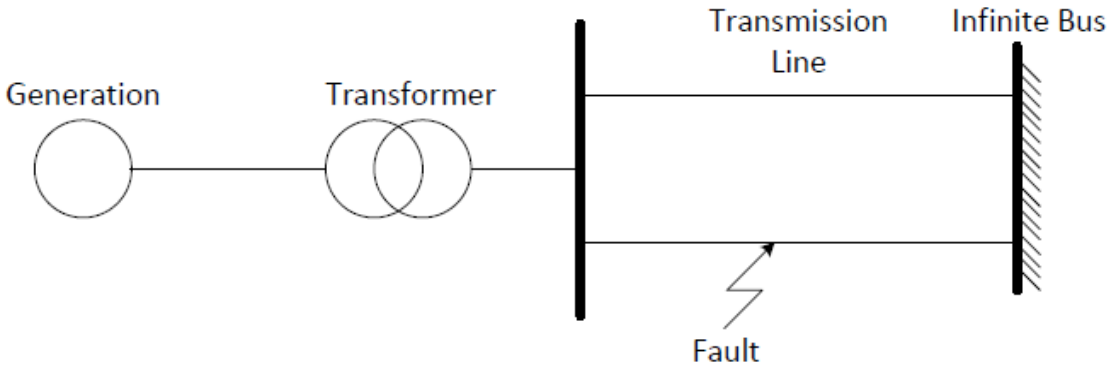

Figure 2.7: Simple SMIB System [19]

Assume that a 3-phase fault appears in the system at $t = 0$ and it is cleared by opening one of the lines. The power angle characteristics of the system are shown in Figure 2.8.

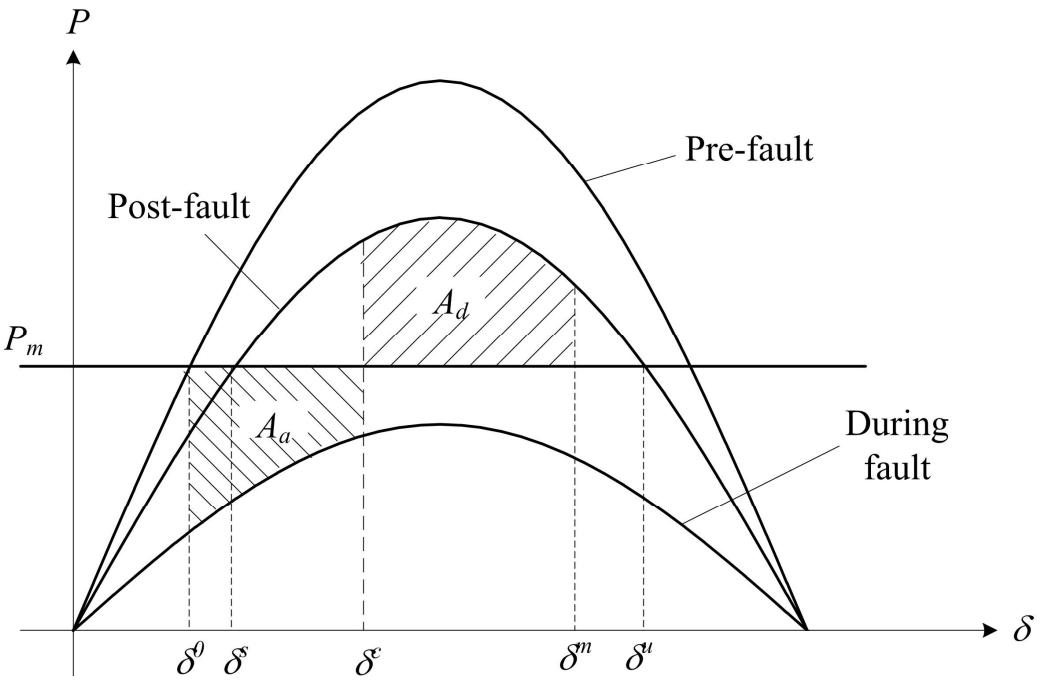

Figure 2.8: Power-Angle Characteristic of the System in Fig. 2.7 [19]

Let δ^0 and δ^s be the pre-fault and post-fault operating or stable-equilibrium points, respectively, of the system. During the fault, the electrical output P_e of the generator reduces drastically (almost to zero) but the mechanical power P_m remains almost constant. Thus the generator accelerates and its angle δ increases. When the fault is cleared by disconnecting the faulted line at time t_c, the output power of the generator becomes greater than the mechanical power and the generator decelerates to bring its speed to normal as shown in Figure 2.8. If the system is stable, the generator will recover to its steady-state speed (or zero speed deviation) at some peak angle δ^m. At δ^m, $P_e > P_m$ and the generator will continue to decelerate. The angle δ decreases from δ^m and reaches a minimum value below δ^s before it starts to increase again. The generator angle will oscillate around δ^s and eventually it will settle down at δ^s because of the system damping. For a given clearing angle δ^c, the peak angle δ^m can be determined by equating the accelerating area A_a to decelerating area A_d. The expressions for A_a and A_d are

$$A_a = \int_{\delta^o}^{\delta^c} \left(P_m - P_e^f \right) d\delta \tag{2.4}$$

$$A_d = \int_{\delta^c}^{\delta^m} \left(P_e^p - P_m \right) d\delta \tag{2.5}$$

where

P_e^f is the during-fault electrical power

P_e^p is the post-fault electrical power

For a system to be transient stable, the maximum decelerating area is greater than the accelerating area. That is, $A_d > A_a$. For a clearing time t_c when $A_d = A_a$, we reach the maximum clearing time referred to as the critical clearing time t_{cr}.

2.2.3 Numerical Integration Methods:

The most commonly used method to solve the swing Equation 2.3 is the numerical integration. The initial condition of the differential equation to be solved is the swing angle δ^o (SEP) of Figure 2.8.

Transient stability analysis is routinely performed in utility system planning. The industry standard for transient stability usually requires the ability of the system to withstand sever disturbances, including any "possible but improbable" three-phase fault close to a generator's Bus. The method used for analysis is time-domain numerical integration. The time-domain numerical integration is not suitable for on-line security analysis due to the long CPU run times for simulation. A typical time-domain numerical integration of 2 seconds takes more than 120 seconds depending on the step size of the integration. Larger step size that reduce time causes inaccurate and less reliable results than smaller step size.

There are different algorithms to perform numerical integration such as trapezoidal rule and Euler integration. Mathematical derivation is illustrated in Chapter 3.

2.2.4 Direct Methods Transient Stability Analysis [1]:

The direct methods determine stability without explicitly solving the system differential equations. This approach has received considerable attention since the early work of Magnusson [8] and Aylett [9] who used transient energy function for stability assessment.

The transient energy approach can be described by considering a ball rolling on the inner surface of a bowl generated by the equation describing the transient energy of the system as depicted in Figure 2.9. The area inside the bowl represents the region of stability and the area outside represents the region of instability. The rim of the bowl represents maximum elevation to δ, and hence, maximum potential energy for the traversed trajectory caused by the fault energy.

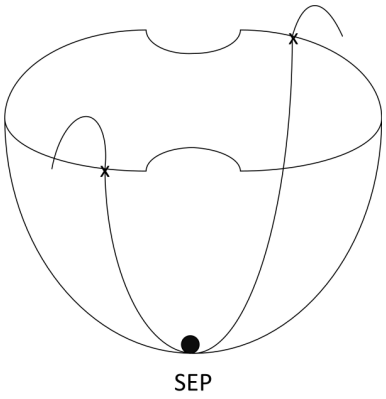

Figure 2.9: A ball rolling on the inner surface of a bowl

Initially, the ball is at rest at the bottom of the bowl, and this state is referred to as the stable equilibrium point (SEP). When the bowl is perturbed, some kinetic energy is injected into the ball causing it to move from its location at SEP in a particular direction. The ball will roll up the inside surface of the bowl along a path determined by the direction of initial motion, and the point where the ball will stop is determined by the amount of the initially injected kinetic energy. If the ball converts all its kinetic energy into potential energy before reaching the rim, then it will

roll back and eventually settle down at the stable equilibrium point again. However, if the injected kinetic energy is high enough to cause the ball to go over the rim, then the ball will enter the region of instability and will not return to the SEP. The surface inside the bowl represents the *potential energy surface* and the rim of the bowl represents the *potential energy boundary surface* (PEBS.)

The application of *transient energy function* (TEF) method to power systems is conceptually similar to that of a rolling ball in a bowl in the hyperspace (n-dimensional space). Initially, the system is operating at steady-state equilibrium point. If a fault occurs, the equilibrium is disturbed causing the synchronous machines to accelerate. The power system gains kinetic energy and potential energy during the fault-on period causing the system to move away from the SEP. After clearing the fault, the kinetic energy is converted to potential energy. For a system to avoid instability, the system must be capable of absorbing the kinetic energy at a time when the forces on the generators tend to bring them toward new equilibrium positions. For a given post-disturbance network configuration, there is a maximum or critical amount of transient energy that the system can absorb. For that reason, assessment of transient stability requires the following:

a) Functions that adequately describe the transient energy responsible for separation of one or more synchronous machines from the rest of the system.
b) An estimate of the critical energy required for the machine to lose synchronism.

Direct methods are suitable for on-line operation for dynamic security assessment because it only requires simple mathematical operations unlike numerical methods which involve solving differential equations numerically. Direct methods may require solving the differential equation up to the point where the fault is cleared. However, there are still some

difficulties in applying direct methods to large power system. The mathematical formulation of the direct methods will be illustrated in Chapter 4.

2.3 Power System Models

In order to analyze any power system, a mathematical model is used to represent the system. It is very important to understand the various power system models before applying them in this thesis. Therefore, several power system models are presented in this section. The models that are presented in this section include: SMIB classical and detailed models, and multi-machine classical model for both synchronous reference frame and center-of-inertia reference frame.

2.3.1 Single-Machine Infinite-Bus System

2.3.1.1 Classical model [1]

Consider the *single-machine infinite-bus* (SMIB) system shown in Figure 2.10.

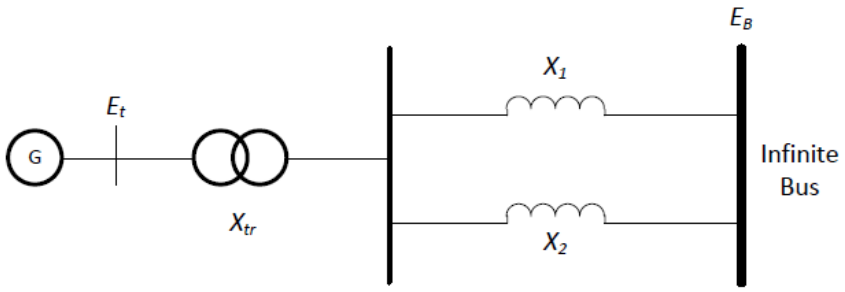

Figure 2.10: Single-machine infinite-bus system [1]

The generator is represented by the classical model, which ignores saliency of round rotor, that is, for the purpose of transient stability, only the transient reactance X_d' is considered with the assumption that the direct and quadrature components are equal. Also, the speed governor effects are neglected. The generator's voltage is denoted by *E'*, and the infinite-bus voltage is denoted by E_B. The rotor angle δ represents the angle by which *E'* leads E_B. When the

system experiences a disturbance, the magnitude of *E'* remains constant at its pre-disturbance value and δ changes as the generator rotor speed deviates from synchronous speed ω_0.

The generator's electrical power output is:

$$P_e = \frac{E'E_s}{X_T}\sin\delta = P_{\max}\sin\delta \tag{2.6}$$

where

$$P_{\max} = \frac{E'E_s}{X_T} \tag{2.7}$$

The equation of motion or the *swing equation* may be written as:

$$\frac{2H}{\omega_0}\frac{d^2\delta}{dt^2} = P_m - P_{\max}\sin\delta \tag{2.8}$$

where

P_m = mechanical power input, in pu

P_{max} = maximum electrical power output, in pu

H = inertia constant, in MW.s/MVA

δ = rotor angle, in elec. rad

t = time, in s

2.3.1.2 Detailed Model [2]

In this model of synchronous machine, the field coil on the direct axis (d-axis) and damper coil on the quadrature axis (q-axis) are considered. The machine differential equations are:

$$\frac{dE'_q}{dt} = \frac{1}{T'_{do}}\left[-E'_q + \left(X_d - X'_d\right)i_d + E_{fd}\right] \tag{2.9}$$

$$\frac{dE'_d}{dt} = \frac{1}{T'_{qo}}\left[-E'_d - \left(X_q - X'_q\right)i_q\right] \tag{2.10}$$

$$\frac{d\delta}{dt} = \omega_B \left(S_m - S_{m0}\right) \tag{2.11}$$

$$\frac{dS_m}{dt} = \frac{1}{2H}\left[T_m - DS_m - T_e\right] \tag{2.12}$$

$$T_e = E_q' i_q + E_d' i_d + \left(X_q - X_q'\right) i_d i_q \tag{2.13}$$

$$E_q' + X_d' i_d - R_a i_q = v_q \tag{2.14}$$

$$E_d' - X_q' i_q - R_a i_d = v_d \tag{2.15}$$

From Equations 2.14 and 2.15, i_d and i_q can be solved as:

$$\begin{bmatrix} i_q \\ i_d \end{bmatrix} = \frac{1}{R_a^2 + X_d' X_q'} \begin{bmatrix} R_a & X_d' \\ -X_q' & R_a \end{bmatrix} \begin{bmatrix} E_q' - v_q \\ E_d' - v_d \end{bmatrix} \tag{2.16}$$

where

T_m = the mechanical torque in the direction of rotation

T_e = the electrical torque opposing the mechanical torque

T_{do}' = d-axis open circuit transient time constant

T_{qo}' = q-axis open circuit transient time constant

S_m = machine slip

S_{m0} = initial machine slip (= *0* in steady-state)

ω_B = the electrical angular frequency

X_d = d-axis reactance

X_q = q-axis reactance

X_d', X_q' = d-axis and q-axis transient reactance, respectively

R_a = armature resistance

E'_d, E'_q = d- and q-axis generator's voltage

i_d, i_q = d- and q-axis current

E_{fd} = control voltage

2.3.2 Multi-machine Infinite-Bus System

2.3.2.1 Synchronous reference frame [11]

For this model, the motion of the generators can be represented by the set of differential equations:

$$\left.\begin{aligned} M_i \dot{\omega}_i + D_i \omega_i &= P_i - P_{ei} \\ \dot{\delta}_i &= \omega_i, \qquad i = 1, 2, ..., n \end{aligned}\right\} \tag{2.17}$$

where, for machine *i*,

δ_i angle of voltage behind transient reactance, indicative of generator rotor position

ω_i rotor speed

M_i generator inertia constant

D_i damping coefficient

The expressions for P_i and P_{ei} are given by:

$$\left.\begin{aligned} P_i &= P_{mi} - E_i^2 G_{ii} \\ P_{ei} &= \sum_{\substack{i=1 \\ j \neq i}}^{n} \left[C_{ij} \sin\left(\delta_i - \delta_j\right) + D_{ij} \cos\left(\delta_i - \delta_j\right) \right] \end{aligned}\right\} \tag{2.18}$$

where

$$C_{ij} = E_i E_j B_{ij}$$
$$D_{ij} = E_i E_j G_{ij}$$

P_{mi} mechanical power input

E_i magnitude of voltage behind transient reactance

G_{ii} real part of the ith diagonal element of the network's Y-matrix

C_{ij}, B_{ij} real and imaginary components of the ijth element of the network's Y-matrix

2.3.2.2 Center of Inertia (COI) Reference Frame **[11]**

The center of inertia model gives a good physical insight into the behavior of synchronous generators. The equation of motion of the generators in the COI reference frame can be represented by:

$$\left.\begin{aligned} M_i \dot{\tilde{\omega}}_i &= P_i - P_{ei} - \frac{M_i}{M_T} P_{COI} - D_i \tilde{\omega}_i \\ \dot{\theta}_i &= \tilde{\omega}_i, \qquad i = 1, \ldots, n \end{aligned}\right\} \tag{2.19}$$

In Equation 2.19, the angle displacement θ_i and angular velocity $\tilde{\omega}_i$ are defined as:

$$\left.\begin{aligned} \theta_i &= \delta_i - \delta_0 \\ \tilde{\omega}_i &= \dot{\theta}_i = \omega_i - \omega_0 \end{aligned}\right\} \tag{2.20}$$

where

$$M_T = \sum_{i=1}^{n} M_i$$

$$\delta_0 = \frac{1}{M_T} \sum_{i=1}^{n} M_i \delta_i$$

$$\omega_0 = \frac{1}{M_T} \sum_{i=1}^{n} M_i \omega_i$$

$$P_{COI} = \sum_{i=1}^{n} \left(P_i - P_{ei} \right)$$

$$\left.\begin{aligned} P_i &= P_{mi} - E_i^2 G_{ii} \\ P_{ei} &= \sum_{\substack{i=1 \\ j \neq i}}^{n} \left[C_{ij} \sin\left(\delta_i - \delta_j \right) + D_{ij} \cos\left(\delta_i - \delta_j \right) \right] \end{aligned}\right\}$$

where

$$C_{ij} = E_i E_j B_{ij}$$
$$D_{ij} = E_i E_j G_{ij}$$

P_{mi} mechanical power input

E_i magnitude of voltage behind transient reactance

G_{ii} real part of the ith diagonal element of the network's Y-matrix

C_{ij}, B_{ij} real and imaginary components of the ijth element of the network's Y-matrix

δ_i and ω_i as defined in Equation 2.17

The center of inertia model will be used later in this thesis.

2.4 Summary:

In this chapter, the basic concepts and definitions of stability in general are discussed. Then, the discussion is focused on the rotor angle stability with its two main types: small-signal stability, and transient stability. After that, a short review of the various methods to analyze transient stability is illustrated which includes: numerical methods, and direct methods which are based on equal area criterion. In addition, power system models are presented for both SMIB and multi machine power systems.

In the next chapter, numerical methods are discussed in details. These methods include: Euler method, Runge-Kutta second- and forth-order methods, and implicit integration method. Also, a method of how to simulate a power system dynamics using matrices is discussed.

CHAPTER 3

TRANSIENT STABILITY USING NUMERICAL METHODS

3.1 Overview:

The differential equations to be solved in power system stability analysis are nonlinear ordinary differential equation with known initial values and can be represented by:

$$\frac{d\mathbf{x}}{dt} = \mathbf{f}\left(\mathbf{x}, t\right) \tag{3.1}$$

where **x** is the state vector of *n* dependent variables and *t* is the independent variable (time). The main goal of numerical integration techniques is to solve for **x**. In this chapter, different numerical integration methods are presented, and a way to simulate a power system with the model in equation 3.1 is illustrated.

3.2 Numerical Integration Methods [1]:

In the following sections, the most commonly used techniques to perform numerical integration are presented.

3.2.1 Euler Method

Consider the first-order differential equation:

$$\frac{dx}{dt} = f\left(x, t\right) \tag{3.2}$$

with $x = x_0$ at $t = t_0$. Figure 3.1 shows the principle of applying the Euler method.

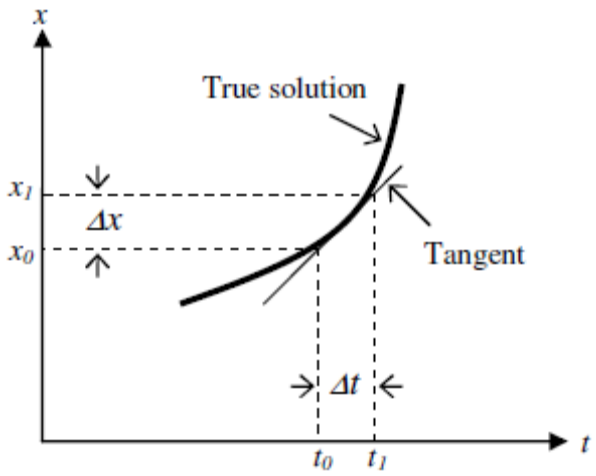

Figure 3.2: Euler's method illustration

At $x = x_0$, $t = t_0$, the curve representing the true solution can be approximated by its tangent having a slope

$$\left.\frac{dx}{dt}\right|_{x=x_0} = f\left(x_0, t_0\right) \tag{3.3}$$

Therefore, the value of x at $t = t_1 = t_0 + \Delta t$ is given by

$$x_1 = x_0 + \Delta x = x_0 + \left.\frac{dx}{dt}\right|_{x=x_0} \cdot \Delta t \tag{3.4}$$

After using the Euler technique for determining $x = x_1$ corresponding to $t = t_1$, another short time step Δt can be taken and x_2 corresponding to $t_2 = t_1 + \Delta t$ can be determined as follows:

$$x_2 = x_1 + \left.\frac{dx}{dt}\right|_{x=x_1} \cdot \Delta t \tag{3.5}$$

The method is also referred to as a *first-order* method because it considers the first derivative in its Taylor series expanded version.

3.2.2 Runge-Kutta (R-K) Methods

3.2.2.1 Second-order R-K Method

The second-order R-K formula for the value of x at $t = t_0 + \Delta t$ is

$$x_1 = x_0 + \Delta x = x_0 + \frac{k_1 + k_2}{2} \tag{3.6}$$

where

$$k_1 = f\left(x_0, t_0\right)\Delta t$$

$$k_2 = f\left(x_0 + k_1, t_0 + \Delta t\right)\Delta t$$

A general formula giving the value of x for the $(n+1)^{st}$ step is

$$x_{n+1} = x_n + \frac{k_1 + k_2}{2} \tag{3.7}$$

where

$$k_1 = f\left(x_n, t_n\right)\Delta t$$

$$k_2 = f\left(x_n + k_1, t_n + \Delta t\right)\Delta t$$

The method is called second-order R-K because it is equivalent to considering up to the second derivative terms of the Taylor series expansion.

3.2.2.2 Forth-order R-K Method

The general formula giving the value of x for the $(n+1)^{st}$ step is

$$x_{n+1} = x_n + \frac{1}{6}\left(k_1 + 2k_2 + 2k_3 + k_4\right) \tag{3.8}$$

where

$$k_1 = f\left(x_n, t_n\right)\Delta t$$

$$k_2 = f\left(x_n + \frac{k_1}{2}, t_n + \frac{\Delta t}{2}\right)\Delta t$$

$$k_3 = f\left(x_n + \frac{k_2}{2}, t_n + \frac{\Delta t}{2}\right)\Delta t$$

$$k_4 = f\left(x_n + k_3, t_n + \Delta t\right)\Delta t$$

The physical interpretation of the above solution is as follows:

k_1 = (slope at the beginning of time step) Δt

k_2 = (first approximation to slope at mid step) Δt

k_3 = (second approximation to slope at mid step) Δt

k_4 = (slope at the end of step) Δt

$\Delta x = 1/6(k_1+2k_2+2k_3+k_4)$

The method is called forth-order R-K because it is equivalent to considering up to the forth derivative terms of the Taylor series expansion.

3.2.3 Implicit Integration Methods

Consider the differential Equation 3.2. The solution for x at $t = t_1 = t_0+\Delta t$ may be expressed in integral form as

$$x_1 = x_0 + \int_{t_0}^{t_1} f\ (x, \tau) d\tau \tag{3.9}$$

Implicit integration methods use interpolation functions for the expression under the integral. The most common implicit integration method is *trapezoidal* rule. The area under the integral of Equation 3.9 is approximated by trapezoids.

The trapezoidal rule for Equation 3.9 is given by

$$x_1 = x_0 + \frac{\Delta t}{2}\left[f\ (x_0, t_0) + f\ (x_1, t_1)\right] \tag{3.10}$$

A general formula giving the value of x at $t = t_{n+1}$ is

$$x_{n+1} = x_n + \frac{\Delta t}{2}\left[f\ (x_n, t_n) + f\ (x_{n+1}, t_{n+1})\right] \tag{3.11}$$

The trapezoidal rule is a second-order method and it is numerically *A-stable*, which means that the stiffness of the system being analyzed affects accuracy but not numerical stability.

Implicit integration methods of higher order have been proposed in the literature on numerical methods; however, they have not been widely used for power system applications especially that they are more difficult to program and less numerically stable than the trapezoidal rule.

When numerical integration methods are used, the system's equations have to be arranged as first-order differential equations.

3.3 Simulation of Power System Dynamic Response

3.3.1 Overall System Equations

Equations for each of the generating units and other dynamic devices may be expressed in the following form:

$$\dot{\mathbf{x}}_d = \mathbf{f}_d\left(\mathbf{x}_d, \mathbf{V}_d\right) \tag{3.12}$$

$$\mathbf{I}_d = \mathbf{g}_d\left(\mathbf{x}_d, \mathbf{V}_d\right) \tag{3.13}$$

where

$\mathbf{x}_d$ = state vector of individual device

$\mathbf{I}_d$ = R and I components of current injection from the device into the network

$\mathbf{V}_d$ = R and I components of bus voltage

Equations 3.12 and 3.13 can be represented using the general form comprising a set of first-order differential equations of Equation 3.14 and a set of algebraic equations of Equation 3.15.

$$\dot{\mathbf{x}} = \mathbf{f}\left(\mathbf{x}, \mathbf{V}\right) \tag{3.14}$$

$$\mathbf{I}\left(\mathbf{x}, \mathbf{V}\right) = \mathbf{Y}_N \mathbf{V} \tag{3.15}$$

where

$\mathbf{x}$ = state vector of the system

$\mathbf{V}$ = bus voltage vector

$\mathbf{I}$ = current injection vector

$\mathbf{Y}_N$ = Y-matrix

3.3.2 Solution of Overall System Equations Using Implicit Integration Methods

The solution of $\mathbf{x}$ at $t = t_{n+1} = t_n + \Delta t$ is given by applying the trapezoidal rule to solve Equation 3.14:

$$\mathbf{x}_{n+1} = \mathbf{x}_n + \frac{\Delta t}{2}\left[\mathbf{f}\left(\mathbf{x}_{n+1}, \mathbf{V}_{n+1}\right) + \mathbf{f}\left(\mathbf{x}_n, \mathbf{V}_n\right)\right] \tag{3.16}$$

From Equation 3.15, the solution of $\mathbf{V}$ at $t = t_{n+1}$ is:

$$\mathbf{I}\left(\mathbf{x}_{n+1}, \mathbf{V}_{n+1}\right) = \mathbf{Y}_N \mathbf{V}_{n+1} \tag{3.17}$$

The vectors $\mathbf{x}_{n+1}$ and $\mathbf{V}_{n+1}$ are unknown. Let

$$\mathbf{F}\left(\mathbf{x}_{n+1}, \mathbf{V}_{n+1}\right) = \mathbf{x}_{n+1} - \mathbf{x}_n - \frac{\Delta t}{2}\left[\mathbf{f}\left(\mathbf{x}_{n+1}, \mathbf{V}_{n+1}\right) + \mathbf{f}\left(\mathbf{x}_n, \mathbf{V}_n\right)\right] \tag{3.18}$$

and,

$$\mathbf{G}\left(\mathbf{x}_{n+1}, \mathbf{V}_{n+1}\right) = \mathbf{Y}_N \mathbf{V}_{n+1} - \mathbf{I}\left(\mathbf{x}_{n+1}, \mathbf{V}_{n+1}\right) \tag{3.19}$$

At solution,

$$\mathbf{F}\left(\mathbf{x}_{n+1}, \mathbf{V}_{n+1}\right) = 0 \tag{3.20}$$

$$\mathbf{G}\left(\mathbf{x}_{n+1}, \mathbf{V}_{n+1}\right) = 0 \tag{3.21}$$

Applying the Newton's method to solve Equations 3.20 and 3.21 iteratively, we get,

$$\begin{bmatrix} \mathbf{x}_{n+1}^{k+1} \\ \mathbf{V}_{n+1}^{k+1} \end{bmatrix} = \begin{bmatrix} \mathbf{x}_{n+1}^{k} \\ \mathbf{V}_{n+1}^{k} \end{bmatrix} + \begin{bmatrix} \Delta\mathbf{x}_{n+1}^{k} \\ \Delta\mathbf{V}_{n+1}^{k} \end{bmatrix} \tag{3.22}$$

Equation 3.23 is solved to obtain $\Delta\mathbf{x}_{n+1}^{k}$ and $\Delta\mathbf{V}_{n+1}^{k}$:

$$\begin{bmatrix} -\mathbf{F}\left(\mathbf{x}_{n+1}^{k}, \mathbf{V}_{n+1}^{k}\right) \\ -\mathbf{G}\left(\mathbf{x}_{n+1}^{k}, \mathbf{V}_{n+1}^{k}\right) \end{bmatrix} = \begin{bmatrix} \dfrac{\partial \mathbf{F}}{\partial \mathbf{x}} & \dfrac{\partial \mathbf{F}}{\partial \mathbf{V}} \\ \dfrac{\partial \mathbf{G}}{\partial \mathbf{x}} & \dfrac{\partial \mathbf{G}}{\partial \mathbf{V}} \end{bmatrix} \begin{bmatrix} \Delta \mathbf{x}_{n+1}^{k} \\ \Delta \mathbf{V}_{n+1}^{k} \end{bmatrix} \tag{3.23}$$

The Jacobian in the Equation 3.23 has the following structure:

$$\mathbf{J} = \begin{bmatrix} \dfrac{\partial \mathbf{F}}{\partial \mathbf{x}} & \dfrac{\partial \mathbf{F}}{\partial \mathbf{V}} \\ \dfrac{\partial \mathbf{G}}{\partial \mathbf{x}} & \dfrac{\partial \mathbf{G}}{\partial \mathbf{V}} \end{bmatrix} = \begin{bmatrix} \mathbf{A}_D & \mathbf{B}_D \\ \mathbf{C}_D & \left(\mathbf{Y}_N - \mathbf{Y}_D\right) \end{bmatrix} \tag{3.24}$$

where

$$\mathbf{A}_D = \begin{bmatrix} \mathbf{A}_{d1} & 0 & \cdots & 0 \\ 0 & \mathbf{A}_{d2} & \cdots & 0 \\ \vdots & \vdots & \ddots & \vdots \\ 0 & 0 & \cdots & \mathbf{A}_{dm} \end{bmatrix} \qquad \mathbf{B}_D = \begin{bmatrix} \mathbf{B}_{d1} \\ \mathbf{B}_{d2} \\ \vdots \\ \mathbf{B}_{dm} \end{bmatrix}$$

$$\mathbf{Y}_D = \begin{bmatrix} \mathbf{Y}_{d1} & 0 & \cdots & 0 \\ 0 & \mathbf{Y}_{d2} & \cdots & 0 \\ \vdots & \vdots & \ddots & \vdots \\ 0 & 0 & \cdots & \mathbf{Y}_{dm} \end{bmatrix} \qquad \mathbf{C}_D = \begin{bmatrix} \mathbf{C}_{d1} & \mathbf{C}_{d2} & \cdots & \mathbf{C}_{dm} \end{bmatrix}$$

A solution to Equations 3.20 and 3.21 can be expressed as follows:

$$\left(\mathbf{Y}_N + \mathbf{Y}_D - \mathbf{C}_D \mathbf{A}_D^{-1} \mathbf{B}_D\right) \Delta \mathbf{V}_{n+1}^{k} = -\mathbf{G}_{n+1}^{k} + \mathbf{C}_D \mathbf{A}_D^{-1} \mathbf{F}_{n+1}^{k} \tag{3.25}$$

3.4 Summary:

In this chapter, four different numerical integration techniques are presented. The first method is Euler method which is represented by Equations 3.4 and 3.5. The second and third methods presented are the second- and forth-order R-K methods which are represented by Equations 3.7 and 3.8, respectively. The forth method presented is the implicit integration methods, and as an example of these methods, trapezoidal rule is illustrated which is represented

by Equation 3.11. Finally, a way of how to simulate a power system dynamic response is discussed and a solution to system dynamics is presented.

In Chapter 4, the second main method of transient stability analysis (direct methods) is discussed and various direct methods based on transient energy function (TEF) are presented. We shall use both step-by-step integration of Chapter 3 and TEF of Chapter 4 to describe the thesis methodology in Chapter 5.

CHAPTER 4

TRANSIENT STABILITY USING DIRECT METHODS

4.1 Overview

In transient stability, the critical clearing time of circuit breakers to clear a fault is the of vital importance when the system is subjected to large disturbances. In real-world application, the critical clearing time can be interpreted in terms of meaningful quantities such as maximum power transfer in the prefault state. The energy-based methods are a special case of the more general Lyapunov's second method or the direct method. The direct methods determine stability without explicitly solving the system differential equations. Energy function methods have proven to be good ways to determine transient stability in a more reliable way than numerical methods. Energy function methods are considered the future of dynamic security assessment [12].

In this chapter, detailed discussion of direct methods assessment of transient stability will be presented.

4.2 Lyapunov's Method [12]

In 1892, A. M. Lyapunov proposed that stability of the equilibrium point of a nonlinear dynamic system of dimension *n* of:

$$\dot{\mathbf{x}} = f\left(\mathbf{x}\right),\ f\left(\mathbf{0}\right) = 0 \qquad (4.1)$$

can be ascertained without numerical integration. Lyapunov's theorem states that if there exists a scaler function *V(x)* for Equation 4.1 that is positive-definite around the equilibrium point "0"

and the derivative $\dot{V}(x) < 0$, then the equilibrium is asymptotically stable. $\dot{V}(x)$ can be obtained as Eqaution 4.2.

$$\dot{V}(x) = \nabla V^T \cdot f(x) \tag{4.2}$$

V(x) is actually a generalization of the concept of the energy of a system. Application of the energy function method to power system stability began with the early work of Magnusson [8] and Aylett [14]. Although many different Lyapunov functions have been tried since then, the first integral of motion, which is the sum of kinetic and potential energies, may have provided the best result. In power literature, Lyapunov's method has become the so-called Transient Energy Function (TEF) method.

4.3 Transient Energy Function Formulation

4.3.1 Main Idea

As previously explained, the transient energy approach can be described by a ball rolling on the inner surface of a bowl as depicted in Figure 2.9. Initially the ball is resting which is equivalent to a power system in its steady-state equilibrium. When an external force is applied to the ball, the ball moves away from the equilibrium point. Equivalently, in a power system, a fault occurs on the system which causes the generator's rotors to accelerate and gain some kinetic energy causing the system to move away from the SEP. If the ball converts all its kinetic energy into potential energy before reaching the rim, then it will roll back and settle down at the SEP eventually. In power systems, after the fault is cleared, the kinetic energy gained during the fault will be converted into potential energy if the system is capable enough to absorb that kinetic energy. Otherwise, the kinetic energy will increase causing the system's machines to lose synchronism and become unstable.

4.3.2 Mathematical Development

From basic mechanics, the sum of potential energy (PE) and kinetic energy (KE) for a conservative system is constant. Thus using well-known formulas for KE and PE, we have an expression for the total energy of the system in terms of the state $\boldsymbol{\delta} = (\delta, \dot{\delta})$:

$$V(\boldsymbol{\delta}) = \frac{1}{2} M \dot{\delta}^2 + \int_{\delta^0}^{\delta} P(u)\,du \tag{4.3}$$

It can be noted that at equilibrium point (i.e., with $\delta = \delta^0$ and $\dot{\delta} = 0$), both the KE and PE are zero. Now, for the power system after time $t \geq T$, that is after the fault is cleared, the system energy is described by Equation 4.4.

$$V(\boldsymbol{\delta}(t)) = \frac{1}{2} M \dot{\delta}_T^2 + \int_{\delta^0}^{\delta_T} P(u)\,du \tag{4.4}$$

The potential energy curve is the key factor in determining the transient stability. In figure 4.1, the potential energy curve is illustrated.

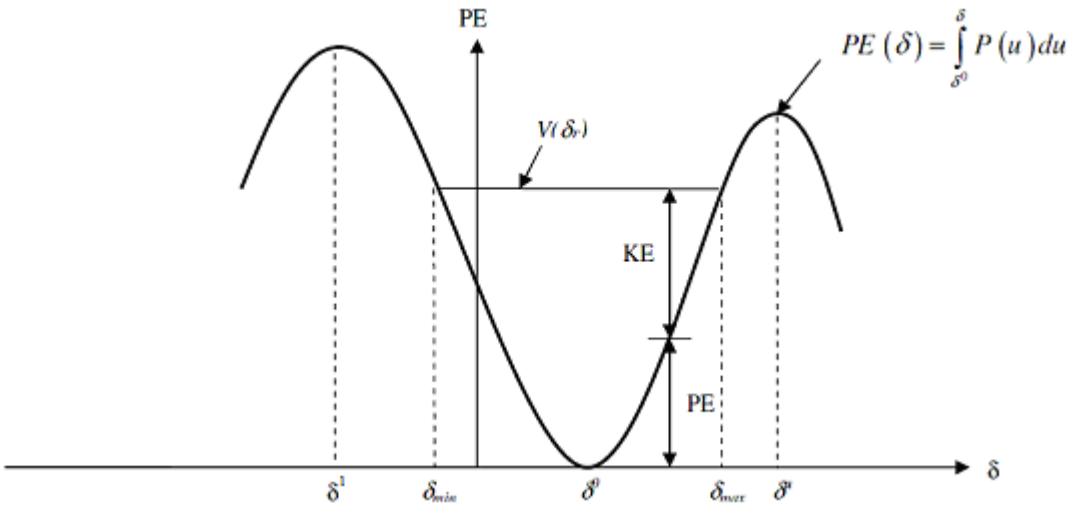

Figure 4.1: Potential energy plot. Redrawn from [7]

From Figure 4.1, the *PE* curve has a local minimum at $\delta = \delta^0$ and has two neighboring local maxima at δ^u and δ^s. Also, the plot shows that if the rotor angle reaches δ_{max}, the system

becomes unstable, that is, if the fault is not cleared before the rotor angle becomes δ_{max}, the trajectory will diverge toward the UEP δ^u. For any $T > T_{critical}$, $\dot{\delta}(t)$ is always positive and $\delta(t)$ increases monotonically with t.

Assume the usual case of a SMIB system, with the generator delivering power. From Equation 4.3 and the definition of PE_{max}, $V(\boldsymbol{\delta}_T) < PE_{max}$ implies that:

$$\frac{1}{2} M \dot{\delta}_T^2 + \int_{\delta^0}^{\delta_T} P(u)du < \int_{\delta^0}^{\delta^u} P(u)du \tag{4.5}$$

The condition of stability is hence:

$$P_m(\delta_T - \delta^0) < \int_{\delta_T}^{\delta^u} P(u)du \tag{4.6}$$

It is more convenient to use Equal Area Criterion to assess stability using TEF. Consider SMIB lossless system depicted in Figure 4.2.

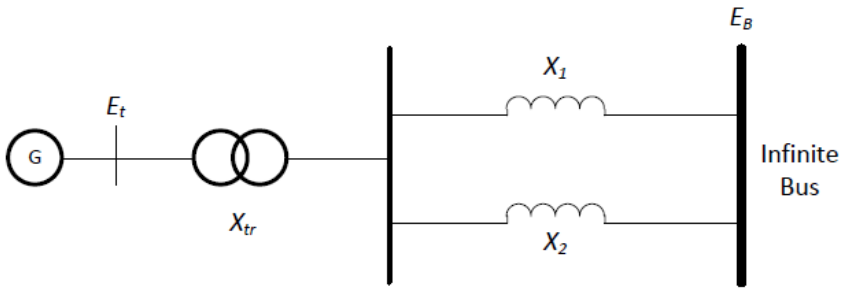

Figure 4.2: SMIB system [1]

A 3-phase fault appears in the system at $t = 0$ and it is cleared by opening one line. The power angle characteristic is shown in Figure 2.8.

4.3.3 Mathematical Development of TEF of Multi-machine Power System

4.3.3.1 Synchronous Reference Frame [18]

Consider the system model represented by Equations 2.17 and 2.18. The TEF V for the synchronous reference frame has the form:

$$V = \sum_{i=1}^{n-1} \sum_{j=i+1}^{n} \left[\frac{1}{2M_T} M_i M_j \left(\omega_i - \omega_j\right)^2 - \frac{1}{M_T} \left(P_i M_j - P_j M_i\right)\left(\delta_{ij} - \delta_{ij}^0\right) \right.$$
$$\left. - C_{ij} \left(\cos\delta_{ij} - \cos\delta_{ij}^0\right) + \int_{\delta_i^0 + \delta_j^0 - 2\delta_o^s}^{\delta_i + \delta_j - 2\delta_o} D_{ij} \cos\delta_{ij} d\left(\delta_i + \delta_j - 2\delta_o\right) \right] \quad (4.7)$$

where in Equation 4.7:

M_i = moment of inertia of machine *i*

ω_i = generator's *i* rotor speed

δ_i = generator's *i* rotor angle

δ_i^0 = generator's *i* SEP

$\delta_{ij} = \delta_i - \delta_j$

$\delta_o = \frac{1}{M_T} \sum_{i=1}^{n} M_i \delta_i$

P_i, C_{ij}, D_{ij} = defined by (2.15)

Equation 4.7 can be used to calculate the total energy of the system after solving for δ_i's numerically. Equation 4.7 consists of four terms: the first term represents the total change in kinetic energy, the second term represents the total change in potential energy, the third term represents the total change in magnetic stored energy, and the fourth term represents the total change in dissipated energy.

***4.3.3.2 Center of Inertia Reference Frame [17]*:**

Consider the system model represented by Equations 2.19 and 2.20. The TEF *V* can be obtained by finding the *n(n-1)/2* relative acceleration equations, multiplying each of these by the corresponding relative velocity and integrating the sum of the resulting equations from a fixed

lower limit of the SEP (denoted by δ^0) to a variable upper limit. Equation 4.8 describes the energy V as a function of angular displacement δ and velocity ω.

$$V = \sum_{i=1}^{n-1}\sum_{j=i+1}^{n}\left[\frac{1}{2M_T}M_i M_j\left(\omega_i-\omega_j\right)^2-\frac{1}{M_T}\left(P_i M_j - P_j M_i\right)\left(\delta_{ij}-\delta_{ij}^0\right)\right.$$
$$\left.-C_{ij}\left(\cos\delta_{ij}-\cos\delta_{ij}^0\right)+\int_{\delta_i^0+\delta_j^0-2\delta_o^s}^{\delta_i+\delta_j-2\delta_o} D_{ij}\cos\delta_{ij}\,d\left(\delta_i+\delta_j-2\delta_o\right)\right] \tag{4.8}$$

Equation 4.8 can be written differently as Equation 4.9.

$$V = 1/2\sum_{i=1}^{n}M_i\tilde{\omega}_i^2-\sum_{i=1}^{n}P_i\left(\theta_i-\theta_i^0\right)$$
$$-\sum_{i=1}^{n-1}\sum_{j=i+1}^{n}\left[C_{ij}\left(\cos\theta_{ij}-\cos\theta_{ij}^0\right)-\int_{\theta_i^0+\theta_j^0}^{\theta_i+\theta_j} D_{ij}\cos\theta_{ij}\,d\left(\theta_i+\theta_j\right)\right] \tag{4.9}$$

where in Equation 4.9,

M_i = moment of inertia of machine i

$\tilde{\omega}_i$ = generator's i rotor speed relative to COI

θ_i = generator's i rotor angle relative to COI

θ_i^0 = generator's i SEP relative to COI

$\theta_{ij} = \theta_i - \theta_j$

P_i, C_{ij}, D_{ij} = defined by (2.15)

The terms of the TEF can be physically interpreted in the following way:

- $KE = 1/2\sum_{i=1}^{n}M_i\tilde{\omega}_i^2 = 1/2\sum_{i=1}^{n}M_i\omega_i^2 - 1/2M_T\omega_o^2$

  Total change in rotor *KE* relative to COI is equal to total change in rotor *KE* minus change in KE_{COI}.

- $PE = \sum_{i=1}^{n} P_i \left(\theta_i - \theta_i^0\right) = \sum_{i=1}^{n} P_i \left(\delta_i - \delta_i^0\right) - \sum_{i=1}^{n} P_i \left(\delta_o - \delta_o^0\right)$

  Given that $\delta_o \triangleq 1/M_T \sum_{i=1}^{n} M_i \delta_i$, change in rotor *PE* relative to COI is equal to the change in rotor potential energy minus change in COI potential energy.

- $C_{ij}\left(\cos\theta_{ij} - \cos\theta_{ij}^0\right)$ is the change in magnetic stored energy of branch *ij*.

- $\int_{\theta_i^0+\theta_j^0}^{\theta_i+\theta_j} D_{ij} \cos\theta_{ij} d\left(\theta_i + \theta_j\right)$ is the change in dissipated energy of branch *ij*.

From the above discussion, it is clear that the change in energy associated with motion of the system COI is subtracted from the total system energy in order to obtain the TEF.

4.4 Multi-machine Transient Stability Measure Using TEF

The multi-machine equal area stability measure is an extension to the well-known Equal Area Criterion (EAC) method, but without considering the SMIB assumption. This stability measure is different from the EAC because it releases some of the assumptions made in the EAC such as, the conductance term could be included in the analysis, and it is used for multi-machine power system analysis without aggregating the system.

In the following sections, a detailed explanation of the use of Transient Energy Function (TEF) to determine stability using the following: TEF for synchronous reference frame, TEF for COI reference frame, and extended equal area criterion (EEAC).

4.4.1 Individual Machine Energy Function for Synchronous Reference Frame [18]

The multi-machine equal area based stability measure is constructed by finding the accelerating and decelerating energy of a particular machine in the power system. To evaluate the accelerating energy, the system is evaluated using the during fault configuration. However, to find the decelerating energy (absorbing energy), the post fault configuration is used.

Additionally, to perform the EAC for a multi-machine system, the critical machine has to be identified. To identify the critical machine (or the most severely disturbed machine SDM), the initial faulted acceleration $d\omega/dt$ is computed for all machines in the system. The SDM can be considered to be the one having the largest faulted acceleration [19]. According to the energy function of Equation 4.7, the potential energy for machine i is:

$$\begin{aligned} V_{PEi}(t) = & \frac{1}{M_T}\sum_{i=1}^{N}\left(P_i M_j - P_j M_i\right)\left(\delta_{ij}(t) - \delta_{ij}^0(t)\right) \\ & + \sum_{\substack{j=1 \\ j\neq i}}^{N} C_{ij}\left(\cos\delta_{ij}(t) - \cos\delta_{ij}^0\right) \\ & - D_{ij}\frac{\delta_i(t) + \delta_j(t) - \delta_i^0 - \delta_j^0}{\delta_i(t) - \delta_j(t) - \delta_i^0 + \delta_j^0}\left[\sin\delta_{ij}(t) - \sin\delta_{ij}^0\right] \end{aligned} \tag{4.10}$$

If machine i is chosen to be the critical generator, the accelerating and decelerating energy of machine i can be used as a stability measure. The accelerating energy at the clearing time t_c is:

$$A_a(t_c) = V_{PEi}(t_c) \tag{4.11}$$

where $V_{Pei}(t)$ depends on the faulted network.

The decelerating energy is:

$$A_d(t, t_c) = V_{PEi}(t) - V_{PEi}(t_c) \tag{4.12}$$

where V_{Pei} depends on the post fault network configuration.

For a given fault-clearing time t_c, the system is considered to be stable if $A_a < A_d$. For a stable system, the SDM reaches the peak angle before the system trajectory reaches the controlling UEP.

Equation 4.10 can be subtracted from the *KE* of generator *i*,

$$V_{KEi} = \frac{1}{2M_T} \sum_{\substack{j=1 \\ j \neq i}}^{N} M_i M_j \left(\omega_i - \omega_j\right)^2 \tag{4.13}$$

which results the total energy of generator *i*. This function is shown to be a Lyapunov function when the conductance term is ignored.

4.4.2 Individual Machine Energy Function for COI Reference Frame

Consider the system model of Equation 2.19. Assume that the effect of damping is neglected in the system since the energy function is used for first swing stability. The following derivation is followed from [20]. By multiplying the *i*th post fault swing equation by $\dot{\theta}_i$ and rearranging, we obtain the expression

$$\left[M_i \dot{\tilde{\omega}}_i - P_i + P_{ei} + \frac{M_i}{M_T} P_{COI} \right] \dot{\theta}_i = 0, \qquad i = 1, ..., n \tag{4.14}$$

Integrating Equation 4.14 with respect to time, using t_0 as a lower limit, where $\dot{\tilde{\omega}}(t_0) = 0$ and $\theta(t_0) = \theta^0$ is the SEP, yields

$$\begin{aligned} V_i = {} & \frac{1}{2} M_i \tilde{\omega}_i^2 - P_i \left(\theta_i - \theta_i^0\right) + \sum_{\substack{j=1 \\ j \neq i}}^{n} C_{ij} \int_{\theta_i^0}^{\theta_i} \sin \theta_{ij} \, d\theta_i \\ & + \sum_{\substack{j=1 \\ j \neq i}}^{n} D_{ij} \int_{\theta_i^0}^{\theta_i} \cos \theta_{ij} \, d\theta_i + \frac{M_i}{M_T} \int_{\theta_i^0}^{\theta_i} P_{COI} \, d\theta_i \end{aligned} \tag{4.15}$$

Equation 4.15 is evaluated using the post fault network configuration. The first term in Equation 4.15 represents the KE of machine *i* with respect to the system COI. The remaining terms are considered to be the PE. Thus, Equation 4.15 can be expressed as:

$$V_i = V_{KEi} + V_{PEi} \tag{4.16}$$

For a given disturbance, transient energy injected into the system during the fault causing the total energy V_i to increase which causes machine *i* to diverge from its equilibrium. When the

fault is cleared, machine's *i* gained *KE* is converted into *PE*. This process continues until the initial *KE* is converted totally into *PE* causing the machine to converge toward the rest of the system. However, if the *KE* of machine *i* is not converted totally into *PE*, machine *i* loses synchronism and separates from the system.

Equation 4.16 consists of two parts: kinetic energy, and potential energy. Both energies need to be solved numerically. After the rotor angles are found numerically, the energies can be represented by:

$$KE_i = \frac{1}{2} M_i \tilde{\omega}_i^2 \tag{4.17}$$

$$\begin{aligned} PE_i = {} & P_i\left(\theta_i - \theta_i^0\right) + \sum_{\substack{j=1 \\ j\neq i}}^{n} C_{ij}\left[\cos\left(\theta_i^0 - \theta_j\right) - \cos\left(\theta_i - \theta_j\right)\right] \\ & + \sum_{\substack{j=1 \\ j\neq i}}^{n} D_{ij}\left[\sin\left(\theta_i - \theta_j\right) - \sin\left(\theta_i^0 - \theta_j\right)\right] + \frac{M_i}{M_T}\int_{\theta_i^0}^{\theta_i} P_{COI}\, d\theta_i \end{aligned} \tag{4.18}$$

$$\begin{aligned} \int_{\theta_i^0}^{\theta_i} P_{COI}\, d\theta_i = {} & \sum_{i=1}^{n}\left(\theta_i - \theta_i^0\right) - \sum_{i=1}^{n}\sum_{\substack{j=1 \\ j\neq i}}^{n} C_{ij}\left[\cos\left(\theta_i^0 - \theta_j\right) - \cos\theta_{ij}\right] \\ & - \sum_{i=1}^{n}\sum_{\substack{j=1 \\ j\neq i}}^{n} D_{ij}\left[\sin\theta_{ij} - \sin\left(\theta_i^0 - \theta_j\right)\right] \end{aligned} \tag{4.19}$$

By using the total energy of the system, part of the boundary of the region of stability is determined by hypersurfaces which passes through the saddle points. These hypersurfaces are from the Potential Energy Boundary Surface (PEBS). At the PEBS, the potential energy is maximum as well as on the boundary of the region of stability. The potential energy close to the UEP is flat. The system maintain stability if the total kinetic energy is converted into potential energy before reaching the PEBS.

Using the preceding discussion, machine *i* remains stable if V_{PEi} is maximum. This maximum value is fairly flat and it is equal to the critical total energy $V_{cr,i}$ of machine *i*.

4.4.3 Extended Equal Area Criterion (EEAC) [19]:

In the derivation of the EEAC, it is assumed that only one machine is severely disturbed and it is responsible for system instability. The other machines are less disturbed and their rotor angles variations are not significant compared to the SDM during the transient period. The SDM can be identified by observing the initial faulted acceleration of the machines.

Let *i* be the critical or SDM for a given disturbance. The dynamics are given by:

$$\left.\begin{aligned} \frac{d\theta_i}{dt} &= \tilde{\omega}_i \\ M_i \frac{d\tilde{\omega}_i}{dt} &= P_{Ai} \end{aligned}\right\} \tag{4.20}$$

where

$$P_{Ai} = a_i - \sum_{\substack{j=1 \\ j\neq i}}^{n} \left(b_{ij} \sin\theta_i + d_{ij} \cos\theta_i \right) \tag{4.21}$$

$$a_i = P_i - \frac{M_i}{M_T} P_T + 2\frac{M_i}{M_T} \sum_{\substack{k=1 \\ k\neq i}}^{n-1} \sum_{\substack{j=k+1 \\ j\neq i}}^{n} D_{kj} \cos\theta_{kj} \tag{4.22}$$

$$b_{ij} = C_{ij} \cos\theta_j + D_{ij} \left(1 - 2\frac{M_i}{M_T} \right) \sin\theta_j \tag{4.23}$$

$$d_{ij} = -C_{ij} \sin\theta_j + D_{ij} \left(1 - 2\frac{M_i}{M_T} \right) \cos\theta_j \tag{4.24}$$

By eliminating the independent variable time *t* in Equation 4.20, the differential relationship between $\tilde{\omega}_i$ and θ_i can be written as:

$$M_i \tilde{\omega}_i d\tilde{\omega}_i = P_{Ai} d\theta_i \tag{4.25}$$

Let us consider the system is critically stable ($t = t_c = t_{cr}$) where t_c and t_{cr} represent clearing and critical clearing times, respectively. For such a system, the post fault trajectory passes near the vicinity of an unstable equilibrium point (UEP) called the controlling UEP. The controlling UEP is the solution of equation to the sum of the squared change in angular speed represented by Equation 4.26 at which $\theta_i > 90^\circ$ and the absolute angle of the rest of the machines is less than 90°:

$$F(\theta) = \sum_{k=1}^{n} \left(P_k - P_{ek} - \frac{M_k}{M_T} P_{COI} \right)^2 = 0 \tag{4.26}$$

Let Equation 4.25 be integrated from the prefault operating point to the post fault controlling UEP:

$$\int_{\omega_i^0=0}^{\omega_i^u=0} M_i \tilde{\omega}_i d\tilde{\omega}_i = \int_{\theta_i^0}^{\theta_i^u} P_{Ai} d\theta_i = 0 \tag{4.27}$$

Note that the change in angular velocity is 0 for all equilibrium points. Now, given that the network changes its configuration at fault clearing (t_c), the right-hand equation of Equation 4.27 can be reconstructed into two parts:

$$\int_{\theta_i^0}^{\theta_i^c} P_{Ai}^f d\theta_i = -\int_{\theta_i^c}^{\theta_i^u} P_{Ai}^p d\theta_i \tag{4.28}$$

The superscripts *f, p,* and *c* represent the faulted, post faulted, and clearing conditions, respectively. The left-hand side of Equation 4.28 is called the accelerating area (energy) A_a and after substitution in the main model of Equation 2.16, we get

$$A_a = \int_{\theta_i^0}^{\theta_i^c} P_{Ai}^f d\theta_i = \int_{\theta_i^0}^{\theta_i^c} \left(P_i^f - P_{ei}^f - \frac{M_i}{M_T} P_{COI}^f \right) d\theta_i \tag{4.29}$$

Equation 4.29 is the equivalent of the so-called integral of accelerating power (P_{Ai}) and it can be solved numerically. Also, it can be represented by the following equation:

$$A_a = \int_{\theta_i^0}^{\theta_i^c} P_{Ai}^f \, d\theta_i = \int_{\theta_i^0}^{\theta_i^c} \left\{ a_i^f - \sum_{\substack{j=1 \\ j \neq i}}^{n} \left(b_{ij}^f \sin\theta_i + d_{ij}^f \cos\theta_i \right) \right\} d\theta_i \qquad (4.30)$$

Since a_i^f , b_i^f and d_i^f are independent of t_i but depend on angles of other machines in the system, a correction factor (the average of sinusoid) is added to convert the integral of Equation 4.30 into summation. Therefore, the accelerating energy becomes:

$$A_a = a_i^f \left(\theta_i^c - \theta_i^0 \right) + \sum_{\substack{j=1 \\ j \neq i}}^{n} \left\{ b_{ij}^f \left(\cos\theta_i^c - \cos\theta_i^0 \right) - d_{ij}^f \left(\sin\theta_i^c - \sin\theta_i^0 \right) \right\} \qquad (4.31)$$

where

$$a_i^f = P_i^f - \frac{M_i}{M_T} P_T^f + 2\frac{M_i}{M_T} \sum_{\substack{k=1 \\ k \neq i}}^{n-1} \sum_{\substack{j=k+1 \\ j \neq i}}^{n} D_{kj}^f \frac{\left(\cos\theta_{kj}^c + \cos\theta_{kj}^0 \right)}{2} \qquad (4.32)$$

$$b_{ij}^f = C_{ij}^f \frac{\left(\cos\theta_j^c + \cos\theta_j^0 \right)}{2} + D_{ij}^f \left(1 - 2\frac{M_i}{M_T} \right) \frac{\left(\sin\theta_j^c + \sin\theta_j^0 \right)}{2} \qquad (4.33)$$

$$d_{ij}^f = -C_{ij}^f \frac{\left(\sin\theta_j^c + \sin\theta_j^0 \right)}{2} + D_{ij}^f \left(1 - 2\frac{M_i}{M_T} \right) \frac{\left(\cos\theta_j^c + \cos\theta_j^0 \right)}{2} \qquad (4.34)$$

Using the same principle, the decelerating area A_d (energy) for the post fault system configuration can be written with just changing the subscripts of *f, c,* and *0* to be *p, u,* and *c*, respectively which represents post fault, UEP, and clearing states. Thus, the decelerating area can be written as:

$$A_d = a_i^p \left(\theta_i^u - \theta_i^c \right) + \sum_{\substack{j=1 \\ j \neq i}}^{n} \left\{ b_{ij}^p \left(\cos\theta_i^u - \cos\theta_i^c \right) - d_{ij}^p \left(\sin\theta_i^u - \sin\theta_i^c \right) \right\} \qquad (4.35)$$

where in Equation 4.35

$$a_i^p = P_i^p - \frac{M_i}{M_T} P_T^p + 2\frac{M_i}{M_T} \sum_{\substack{k=1 \\ k \neq i}}^{n-1} \sum_{\substack{j=k+1 \\ j \neq i}}^{n} D_{kj}^p \frac{\left(\cos\theta_{kj}^u + \cos\theta_{kj}^c\right)}{2} \tag{4.36}$$

$$b_{ij}^p = C_{ij}^p \frac{\left(\cos\theta_j^u + \cos\theta_j^c\right)}{2} + D_{ij}^p \left(1 - 2\frac{M_i}{M_T}\right) \frac{\left(\sin\theta_j^u + \sin\theta_j^c\right)}{2} \tag{4.37}$$

$$d_{ij}^p = -C_{ij}^p \frac{\left(\sin\theta_j^u + \sin\theta_j^c\right)}{2} + D_{ij}^p \left(1 - 2\frac{M_i}{M_T}\right) \frac{\left(\cos\theta_j^u + \cos\theta_j^c\right)}{2} \tag{4.38}$$

For the case of SDM, the critical clearing time occurs when the accelerating area equals to the decelerating area ($A_a = A_d$); the SDM reaches the zero speed deviation when the fault is cleared exactly on the critical clearing time. However, if the SDM cannot reach the zero speed deviation when its angle reaches the value θ_i^u, the system considered to be unstable. This happens when $t_c > t_{cr}$. For a given fault clearing time t_c, the system is considered to be stable if $A_a < A_d$.

4.4.4 Proposed Method:

The proposed method in the thesis is based on the single-machine energy function explained in sections 4.4.1 and 4.4.2. Since the focus of this thesis is on the COI, the method is explained for the COI only. At first, the system is separated into two groups: the severely disturbed group, and the less disturbed group. Each of the groups has to consist of at least two machines. Let *SDG* be the number of severely disturbed machines, where $2 \leq SDG < n$. In order to determine the *SDG*, a tolerance is set by the user such that,

$$SDG = \left\{ i : \max_{1 \leq i \leq n} |\alpha_i| - |\alpha_i| \leq \text{tolerance} \right\} \tag{4.39}$$

where,

$$\alpha_i = \left(P_i - P_{ei} - \frac{M_i}{M_T} P_{COI} \right) M_i^{-1} \tag{4.40}$$

After the *SDG* is determined, the kinetic energy of the clearing instant of the generators at *SDG* is calculated using Equation 4.17. The calculated kinetic energies are added together as follows:

$$KE_{SDG} = \frac{1}{2} \sum_{i=1}^{length(SDG)} M_{SDG(i)} \omega_{SDG(i)}^2 \tag{4.41}$$

where,

SDG(i) means the machine number of the *SDG*, that is, *i* works as an index to the *SDG* set

After determining the kinetic energies of the *SDG*, the potential energies of each machine in the system are calculated using the post-fault configuration using Equations 4.18 and 4.19. Depending on the length of the set *SDG*, the same number of machines is used to sum the smallest resulting potential energies. To calculate the potential energy, θ_i^0 and θ_i in Equations 4.18 and 4.19 are replaced by θ_i^s and θ_i^c, respectively. That is,

$$PE_{SDG} = \sum_{i=1}^{length(SDG)} PE_i \left(\theta_i^s, \theta_i^c \right) \tag{4.42}$$

after sorting the potential energies from the smallest to the largest. The two values are compared and based on the comparison a decision on stability can be made. If $PE_{SDG} > KE_{SDG}$, then the system is considered stable. Otherwise, the system is unstable. If $PE_{SDG} = KE_{SDG}$, then the system is critically stable.

4.5 Summary:

In this chapter, detailed discussion of direct methods is provided. A brief discussion of Lyapunov's method is presented. Lyapunov's method introduces the energy function of a power system that can be used in stability studies. Then, transient energy function (TEF) is discussed

and mathematical formulation is provided. The more specific case of the multi-machine energy function is developed for both the synchronous reference frame and the COI reference frame. Also, the extended equal area criterion for the severely disturbed machine is discussed and the mathematical formulation is developed. Finally, the proposed method is explained briefly for the COI reference frame. Algorithm of the proposed method is provided in Chapter 6.

In Chapter 5, the IEEE 39 Bus equivalent power system is introduced and all its parameters are presented. The IEEE 39 Bus system is used for testing and verifying the performance of the proposed method.

CHAPTER 5

TEST SYSTEM

5.1 IEEE 39 Bus Test System:

The IEEE 39 Bus (New England) power system is an equivalent power system of subsystems of the New England area and Canada. It consists of 39 Buses of which 10 Buses are generator Buses, 12 transformers, 10 generators, 34 transmission lines, and 19 loads. The system is shown in Figure 5.1. In this section of the chapter, the test data and parameters are introduced to be used to simulate the various methods of transient stability analysis.

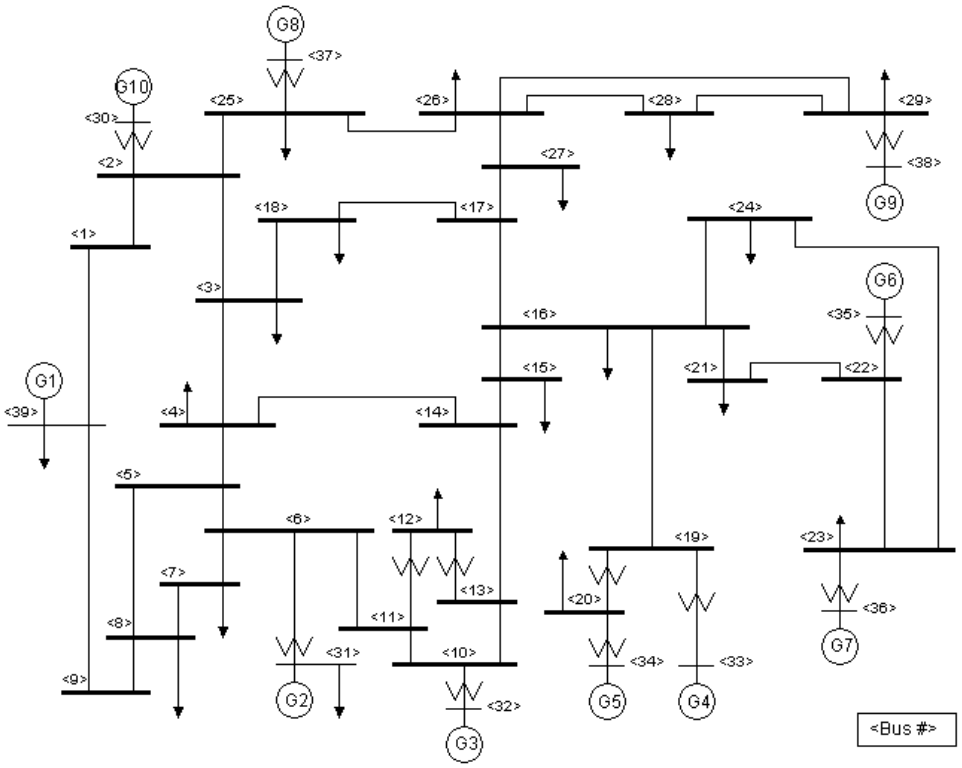

Figure 5.1: IEEE 39 Bus System [21]

5.1.1 Transmission Lines:

The IEEE 39 Bus system contains 34 transmission lines. Each transmission line has different length with different resistance, reactance, and suceptance per unit length depending on the material. However, since the length of transmission line does not affect the analysis in this thesis, only the per unit parameters are presented in Table 5.1.

Table 5.1: Transmission Line Data

Line	Resistance PU	Reactance PU	Suceptance PU	Line	Resistance PU	Reactance PU	Suceptance PU
1 to 2	0.0035	0.0411	0.6987	13 to 14	0.0009	0.0101	0.1723
1 to 39	0.0010	0.0250	0.7500	14 to 15	0.0018	0.0217	0.3660
2 to 3	0.0013	0.0151	0.2572	15 to 16	0.0009	0.0094	0.1710
2 to 25	0.0070	0.0086	0.1460	16 to 17	0.0007	0.0089	0.1342
3 to 4	0.0013	0.0213	0.2214	16 to 19	0.0016	0.0195	0.3040
3 to 18	0.0011	0.0133	0.2138	16 to 21	0.0008	0.0135	0.2548
4 to 5	0.0008	0.0128	0.1342	16 to 24	0.0003	0.0059	0.0680
4 to 14	0.0008	0.0129	0.1382	17 to 18	0.0007	0.0082	0.1319
5 to 6	0.0002	0.0026	0.0434	17 to 27	0.0013	0.0173	0.3216
5 to 8	0.0008	0.0112	0.1476	21 to 22	0.0008	0.0140	0.2565
6 to 7	0.0006	0.0092	0.1130	22 to 23	0.0006	0.0096	0.1846
6 to 11	0.0007	0.0082	0.1389	23 to 24	0.0022	0.0350	0.3610
7 to 8	0.0004	0.0046	0.0780	25 to 26	0.0032	0.0323	0.5130
8 to 9	0.0023	0.0363	0.3804	26 to 27	0.0014	0.0147	0.2396
9 to 39	0.0010	0.0250	1.2000	26 to 28	0.0043	0.0474	0.7802
10 to 11	0.0004	0.0043	0.0729	26 to 29	0.0057	0.0625	1.0290
10 to 13	0.0004	0.0043	0.0729	28 to 29	0.0014	0.0151	0.2490

The above data are in per unit system at base voltage of *345 kV* and *100 MVA*. The resistance, impedance and suceptance are given for the total length of transmission lines.

5.1.2 Transformers:

The transformers data consists of R_T (Resistance) and X_T (Reactance) which are the equivalent of the primary and secondary windings of the transformer. The following table provides the transformers parameters.

Table 5.2: Transformers Data

Line Data				Transformer Tap	
From Bus	**To Bus**	R_T	X_T	**Magnitude**	**Angle**
12	11	0.0016	0.0435	1.0060	0.0000
12	13	0.0016	0.0435	1.0060	0.0000
6	31	0.0000	0.0250	1.0700	0.0000
10	32	0.0000	0.0200	1.0700	0.0000
19	33	0.0007	0.0142	1.0700	0.0000
20	34	0.0009	0.0180	1.0090	0.0000
22	35	0.0000	0.0143	1.0250	0.0000
23	36	0.0005	0.0272	1.0000	0.0000
25	37	0.0006	0.0232	1.0250	0.0000
2	30	0.0000	0.0181	1.0250	0.0000
29	38	0.0008	0.0156	1.0250	0.0000
19	20	0.0007	0.0138	1.0600	0.0000

All the above data are in per unit based on *20 kV* for the primary windings and *345 kV* for the secondary.

5.1.3 Generators:

There are 10 generators in the system. The 10 generators are connected to Bus 30 through Bus 39. Bus 31 is considered a slack Bus, while the remaining 9 are called PV Buses. The 29 remaining Buses are all called PQ Buses.

The following table gives the initial load flow conditions of the 10 generators Buses. All the values are based on *100 MVA* and the machines rated terminal voltages.

Table 5.3: Generators' Initial Load Flow

Bus	Generator	Rated Voltage kV	Voltage PU	Active Power PU
30	10	20	1.0475	2.50
31	2	20	0.9820	Slack Generator
32	3	20	0.9831	6.50
33	4	20	0.9972	6.32
34	5	20	1.0123	5.08
35	6	20	1.0493	6.50
36	7	20	1.0635	5.60
37	8	20	1.0278	5.40
38	9	20	1.0265	8.30
39	1	345	1.0300	10.00

The following table gives the generators' rated voltage, inertia, resistance, leakage reactance, transient and sub-transient reactance's, and time constants.

Table 5.4: Generators Details

GEN	R_a	X_l	X_d	X_q	X'_d	X'_q	X''_d	X''_q	T'_{d0}	T'_{q0}	T''_{d0}	T''_{q0}	*H(s)*
1	0	0.0030	0.2000	0.0190	0.0060	0.0080	0.0006	0.0006	7.0000	0.7000	0.0330	0.0563	500.0
2	0	0.0350	0.2950	0.2820	0.0697	0.1700	0.0369	0.0369	6.5600	1.5000	0.0660	0.0660	30.3
3	0	0.0304	0.2495	0.2370	0.0531	0.0876	0.0320	0.0320	5.7000	1.5000	0.0570	0.0570	35.8
4	0	0.0295	0.2620	0.2580	0.0436	0.1660	0.0310	0.0310	5.5900	1.5000	0.0570	0.0570	28.6
5	0	0.0540	0.6700	0.6200	0.1320	0.1660	0.0568	0.0568	5.4000	0.4400	0.0540	0.0540	26.0
6	0	0.0224	0.2540	0.2410	0.0500	0.0814	0.0236	0.0236	7.3000	0.4000	0.0730	0.0730	34.8
7	0	0.0322	0.2950	0.2920	0.0490	0.1860	0.0340	0.0340	5.6600	1.5000	0.0560	0.0560	26.4
8	0	0.0280	0.2900	0.2800	0.0570	0.0911	0.0300	0.0300	6.7000	0.4100	0.0670	0.0670	24.3
9	0	0.0298	0.2106	0.2050	0.0570	0.0587	0.0314	0.0314	4.7900	1.9600	0.0470	0.0470	34.5
10	0	0.0125	0.1000	0.0690	0.0310	0.0180	0.0132	0.0132	10.2000	0.3000	0.1000	0.1000	42.0

5.1.4 Loads:

The loads of this system are represented by fixed impedance for the purpose of this thesis. The following table shows the data of the 19 loads of the system.

Table 5.5: Loads Data

Bus	Rated Voltage kV	Load MW	Load MVAR	Bus	Rated Voltage kV	Load MW	Load MVAR
3	345	322	2.4	23	345	247.5	84.6
4	345	500	184	24	345	308.6	-92.2
7	345	233.8	84	25	345	224	47.2
8	345	522	176	26	345	139	17
12	345	7.5	88	27	345	281	75.5
15	345	320	153	28	345	206	27.6
16	345	329	32.3	29	345	283.5	26.9
18	345	158	30	31	20	9.2	4.6
20	345	628	103	39	345	1104	250
21	345	274	115				

5.2 Summary:

In this chapter, the IEEE 39 Bus power system is introduced and all its parameters are provided. As previously stated, the system consists of 39 Buses, 12 transformers, 10 generators, 34 transmission lines, and 19 loads. The transmission lines parameters are given in the standard per unit as well as the transformers and generators. For the purpose of this thesis, the loads are represented by fixed impedances. This system will be used to test and simulate previous methods and proposed method of transient stability.

In Chapter 6, PSAT for MATLAB is introduced to be used for the simulation. The simulation of four methods is performed and the results are tabulated. The four methods are: transient stability using numerical methods, TEF for COI reference frame using critical potential energy, EEAC, and the proposed method.

CHAPTER 6

SIMULATION AND RESULTS

6.1 Methodology:

6.1.1 Energy Conversion Comparison for Single Machine:

The method we proposed is based on individual machine energy function. In a SMIB power system, the EAC is used to assess the transient stability on a fault occurrence. The EAC for a SMIB is based on comparing the kinetic energy of the machine on the clearing time instant with the absorbing potential energy from the clearing instant to the controlling UEP. The stability criterion is that if the system's kinetic energy is less than the potential energy, then the system is stable. The multi machine power system using single machine energy function uses the same principle. However, because there are more than one machine in the system, then the generator with the largest kinetic energy at the fault clearing instant and the generator with the smallest potential energy calculated from the rotor angles at the clearing instant to the controlling UEP are used for the comparison.

Algorithm:

i. Set up the parameters of the system and the used model of the system. The Y-matrix must be saved for later usage.

ii. Run power flow calculations to determine the steady-state values of the system.

iii. Run time domain (TD) numerical simulation from the fault occurrence to the fault clearing instant using any method explained in Chapter 3. In this simulation, forward Euler method is used.

iv. Save all generators' voltages, rotor angles, and rotors' speeds.

v. For the Y-matrix, replace all rows and column of the faulted Bus by zeros "0", and perform Kron reduction until a 10×10 matrix is resulted.

vi. Using the post-fault configuration (by replacing the disconnected line in the Y-matrix by 0's), use Kron reduction until a 10×10 matrix is resulted.

vii. Use the appropriate equation to determine the kinetic and potential energies. For COI reference frame analysis, use Equations 4.17 - 4.19, and for synchronous reference frame, use Equations 4.10 and 4.13 if the classical model is used. If the detailed model is used (which is rare for direct methods), then more advanced equations can be used which are found in [2].

viii. Sort the kinetic energies for the single machines in descending order while the potential energy in ascending order.

ix. Use Equation 4.20 to find sectors of severely disturbed machines using an appropriate tolerance depending on the size of the system.

x. Compare the largest kinetic energy sector with the sector of smallest potential energy. If the sector of largest kinetic energy is greater than the smallest potential energy, then the system is unstable. Otherwise, the system is stable.

6.1.2 Determining Critical Clearing Time

In this section, an algorithm to search for the critical clearing time is presented.

Algorithm:

i. Start the process by setting up a fault with 0 seconds clearing time.

ii. Set up PSAT accordingly.

iii. Choose an acceptable error tolerance. The error is the difference between the kinetic energy and the potential energy. In this research, 0.01 is used.

iv. Run power flow in order to get the initial system's dynamic parameters.

v. Set a multiplier α to 1. That is, α is used to control the clearing time depending on this equation:

$$t_c^{(i+1)} = \alpha t_c^{(i)}$$

The technique of determining α is explained in a later step of this algorithm.

vi. Start the search using "do-while" loop.

vii. Run step-by-step integration.

viii. Save θ_i and $\tilde{\omega}_i$ for all generators as well as the Y-matrix.

ix. Perform the Kron reduction to get the reduced Y-marix.

x. Determine the SDG, then calculate the potential and kinetic energies.

xi. Sort the KE and PE in descending and ascending order, respectively.

xii. Find the error. The error is found using this equation:

$$error = PE_{SDG} - KE_{SDG}$$

xiii. If the absolute error is greater than the tolerance, then calculate α (from step xiv) and go to step vi. Otherwise, stop.

xiv. To calculate α, use any appropriate technique to determine the optimal α. In this research, although the search technique is not carefully studied, the following if-else procedure is used:

if $error \geq 1$

$\alpha = 1.2\alpha$

else if $error < 1 \quad \&\& \quad error \geq 0.5$

$\alpha = 1.05\alpha$

else if $error < 0.5 \quad \&\& \quad error \geq 0.2$

$\alpha = 1.01\alpha$

else if $error < 0.2 \quad \&\& \quad error > 0$

$\alpha = 1.001\alpha$

else if $error < 0$

$\alpha = \alpha - 0.02$

end

This algorithm can be represented using the flow chart in Figure 6.1. From the flow chart, the process starts with initializing the process to perform forward Euler method for time-domain analysis for the COI reference frame. Then power flow is run in order to get the initial steady-state values of the dynamic parameters (rotor speed and angle for classical model). After that, the time-domain (step-by-step) integration is run up to the clearing instant with a step size of 10^{-3} seconds that is set in the initialization stage. After saving the results, the critical group (or SDG) is determined using a subroutine called SDG. The function SDG calculates the absolute acceleration and groups the generators into two groups: SDG group, and less disturbed group. Only the SDG is returned. Then, the kinetic energies of the SDG is compared with the smallest potential energies in the system. If the difference between the kinetic energy and potential energy is greater than the tolerance, then the clearing time is incremented using procedure explained in step xiv of the above algorithm. The process time-domain analysis is run again and same process is done until the criterion is met. The criterion is the error tolerance that is set in the initialization stage. Once again, the incrementing process may not be the best technique, but it was efficient enough for the purpose of this thesis.

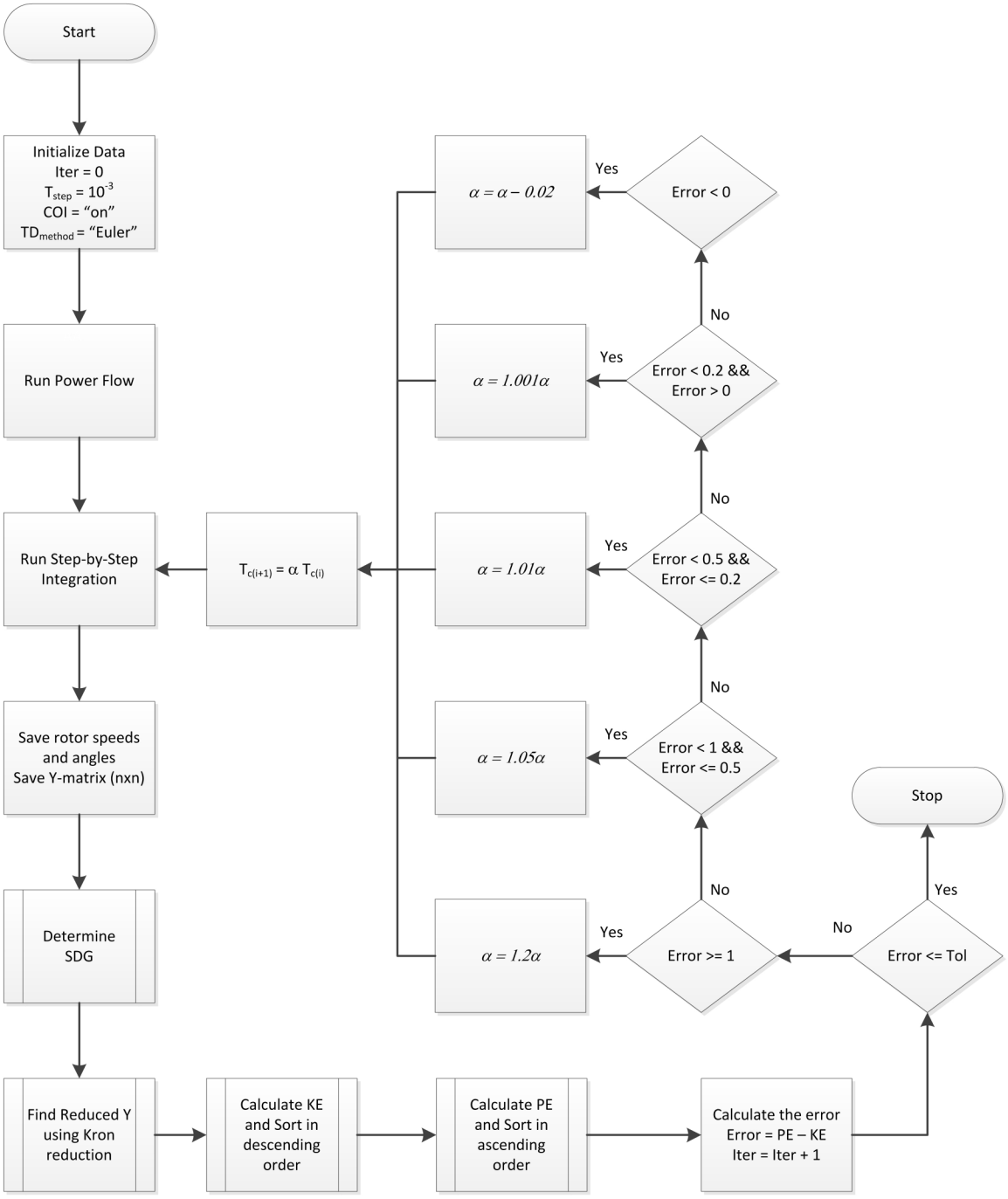

Figure 6.1: Flow chart of the proposed method applied to IEEE 39 Bus System

6.2 Power System Analysis Toolbox (PSAT) in MATLAB:

6.2.1 Overview:

PSAT is a MATLAB toolbox for electric power system analysis and control. PSAT is open source package. It has been developed using MATLAB by Professor Federico Milano.

According to Dr. Milano, PSAT is the first free software project in the field of power system analysis. Also, PSAT is the first power system software which runs on GNU/Ovtave platforms. PSAT kernel is the power flow algorithm, which also initiate the state variables. After the power flow is solved, the user can perform further static and/or dynamic analyses such as, small-signal stability analysis, time-domain simulation, optimal power flow (OPF), and continuation power flow (CPF).

PSAT uses MATLAB vectorized computations and sparse matrix functions in order to optimize performances. PSAT also is provided with the most complete set of algorithms for static and dynamic analyses among currently available MATLAB-based power system software [10].

PSAT supports a variety of static and dynamic models as follows [10]:

- *Power Flow Data*: Bus bars, transmission lines and transformers, slack Buses, PV generators, constant power loads, and shunt admittance.
- *Market Data*: Power supply bids and limits, generator power reserves, and power demand bids and limits.
- *Switches*: Transmission line faults and breakers.
- *Measurements*: Bus frequency measurements.
- *Loads*: Voltage dependent loads, frequency dependent loads, ZIP (polynomial) loads, thematically controlled loads, and exponential recovery loads.
- *Machines*: Synchronous machines and induction motors.
- *Controls*: Turbine Governors, AVRs, PSSs, over-excitation limiters, and secondary voltage regulations.

6.2.2 Models and Algorithms for Numerical Simulation:

6.2.2.1 Power System Model:

The standard power system model is a set of non-linear differential equation as follows:

$$\begin{aligned} \dot{x} &= f\left(x, y, p\right) \\ 0 &= g\left(x, y, p\right) \end{aligned} \tag{6.1}$$

where x are the state variables $x \in \mathbb{R}^n$; y are the algebraic variables $y \in \mathbb{R}^m$; p are the independent variables $p \in \mathbb{R}^l$; f are the differential equations $f : \mathbb{R}^n \times \mathbb{R}^m \times \mathbb{R}^l \to \mathbb{R}^n$; and g are the algebraic equations $g : \mathbb{R}^m \times \mathbb{R}^m \times \mathbb{R}^l \to \mathbb{R}^m$.

PSAT uses Equation 6.1 in all algorithms. The algebraic equations g are obtained as the sum of all active and reactive power injections at buses as in Equation 6.2.

$$g\left(x, y, p\right) = \begin{bmatrix} g_p \\ g_q \end{bmatrix} = \begin{bmatrix} g_{pm} \\ g_{qm} \end{bmatrix} - \sum_{c \in \mathcal{C}_m} \begin{bmatrix} g_{pc} \\ g_{qc} \end{bmatrix} \quad \forall_m \in \mathcal{M} \tag{6.2}$$

where g_{pm} and g_{qm} are the power flows in transmission lines, $\mathcal{M}$ is the set of network buses, $\mathcal{C}_m$ and $\left[g_{pc}^T, g_{qc}^T\right]^T$ are the set of the power injections of components connected at bus m, respectively.

6.2.2.2 Power Flow

The power flow problem is formulated as (6.1) with zero first time derivatives:

$$\begin{aligned} 0 &= f\left(x, y\right) \\ 0 &= g\left(x, y\right) \end{aligned} \tag{6.3}$$

PSAT includes the standard Newton-Raphson method, the fast decoupled power flow, and a power flow with a distributed slack bus model. The power flow model is solved using the methods included depending on the user's preference.

6.2.2.3 Time-Domain Simulation:

There are two integration methods available in PSAT: backward Euler which is explained by Equation 3.5, and trapezoidal rule that is A-stable algorithm which is explained by Equation 3.11. According to the author, PSAT is the only MATLAB-based tool which implements a simultaneous-implicit method for the numerical integration [10] of the model in Equation 6.1.

6.3 Simulation Results

To test the suggested method of transient stability assessment of the IEEE 39 Bus equivalent power system using single machine kinetic and potential energies comparison, the system is built using PSAT. The system is built using built-in PSAT and MATLAB functions rather than using built-in PSAT blocks in Simulink.

At first, the power flow is run and the results are compared with those of [2]. After that, a fault is set and cleared afterward. The time simulation is stopped at the clearing instant because the direct methods do not require any result after the clearing time. The various methods of direct methods are used and compared in the following sections.

6.3.1 Power Flow Results Using PSAT:

After setting up the IEEE 39 equivalent power system in PSAT, power flow is run using Newton-Raphson's method. Due to the length of the obtained report, it is documented in Appendix A.3.

6.3.2 Numerical Simulation in PSAT

PSAT uses two different methods: forward Euler method, and trapezoidal rule. The two methods are simulated for 5 seconds with two different fault locations. At first, the classical model of the power system is used. A 3-phase fault is applied on Bus 15 and it is cleared after

14/60 seconds. The following is a plot of the generators rotors' speeds and angles relative to the COI using forward Euler method.

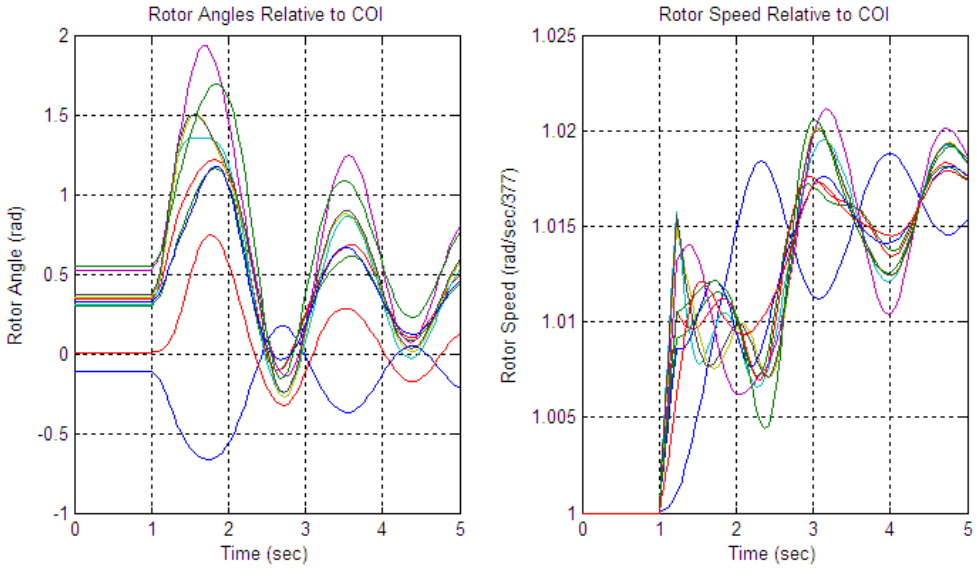

Figure 6.2: Rotors' speeds and angles relative to COI using forward Euler's method plots

Figure 6.2 contains ten curves in each plot. Each curve represents the rotor's speed and angle of a single generator in the system.

Now, for the same system and the same fault, Trapezoidal rule is used and the following plots are obtained.

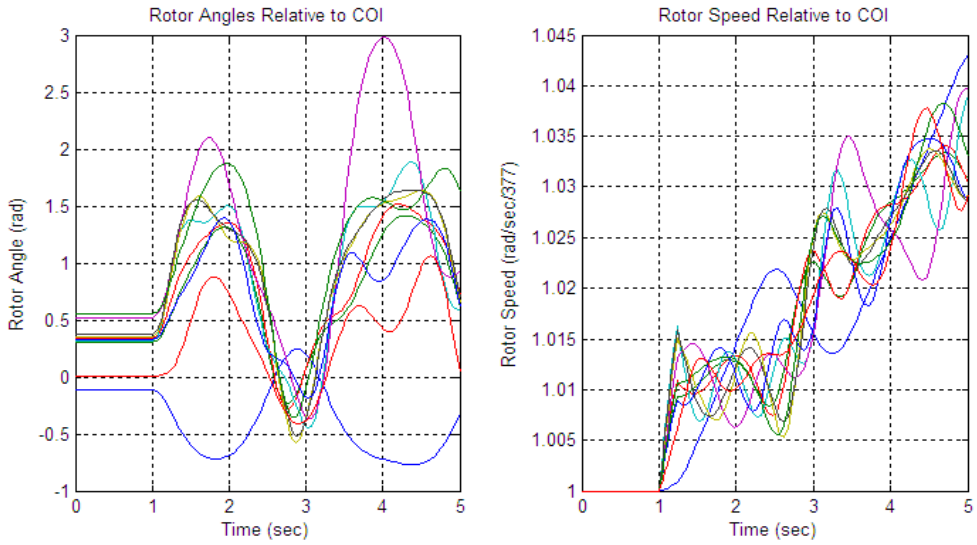

Figure 6.3: Rotors' speeds and angles relative to COI using Trapezoidal rule plots

Figure 6.3 shows two plots of the rotors' angles and speeds of each of the ten generators in the 39-Bus system obtained by using Trapezoidal rule.

The plots in Figures 6.2 and 6.3 cannot be compared, so another plot with one generator only (say generator 2) is plotted to verify the performance of both methods.

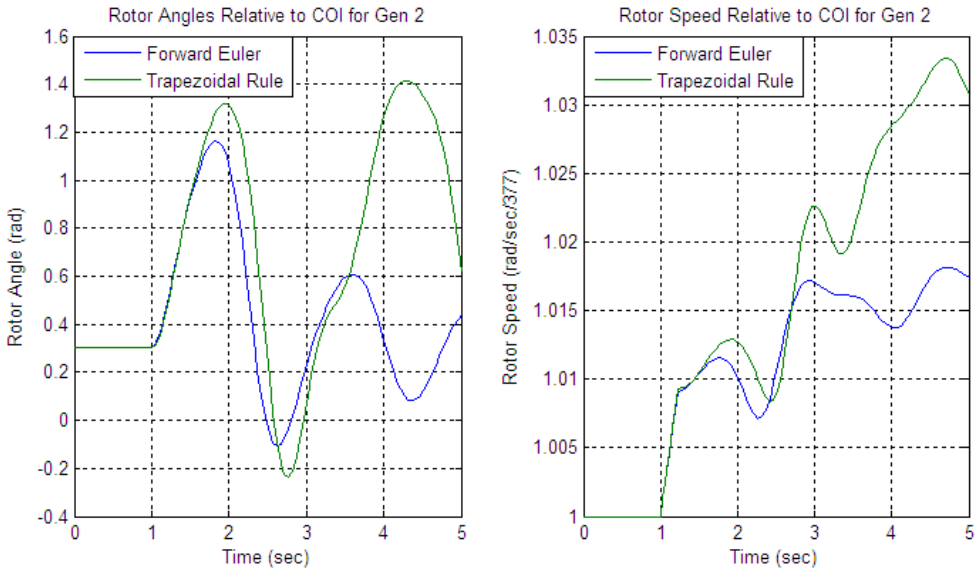

Figure 6.4: Obtained plots of generator 2 rotor's angle and speed using forward Euler and Trapezoidal rule

As seen in Figure 6.4, both methods give approximately similar results. In this thesis, forward Euler method is used for all numerical simulations.

Using the same settings, another numerical simulation using forward Euler is performed for synchronous reference frame instead of COI reference frame. The rotors' angles and speeds relative to the synchronous reference frame of each of the ten generators in the test system are captured and plotted in Figure 6.5.

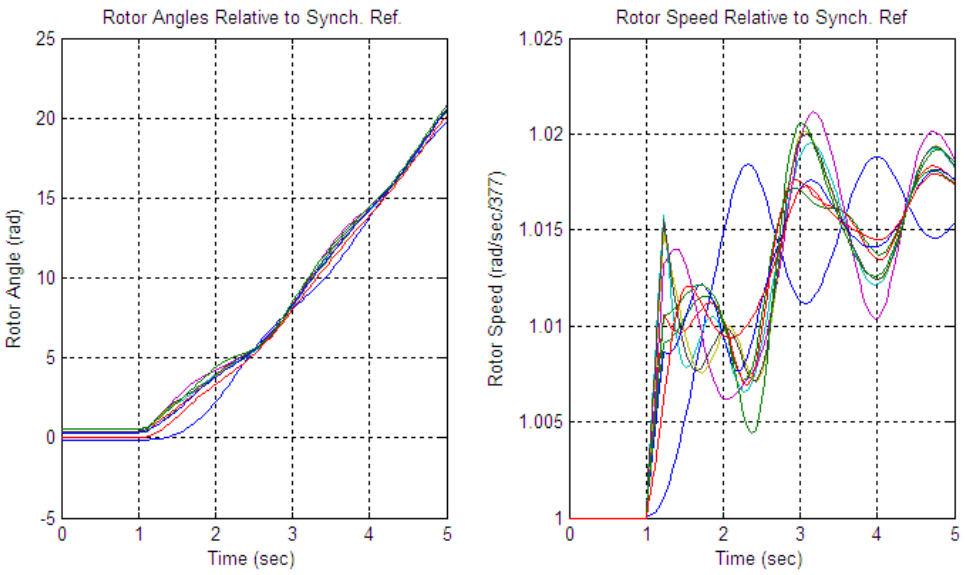

Figure 6.5: Rotors' angles and speeds relative to synchronous reference frame plots using forward Euler

6.3.3 Kron Reduction of Y-matrix

In order to perform the proposed method to the 39 Bus power system, the 39×39 admittance matrix has to be converted into 10×10 equivalent matrix. To perform the reduction, Kron reduction is used.

For an *n*-bus system, if node *k* has zero current injection, then we can obtain the reduced admittance matrix by eliminating node *k* by using the formula:

$$Y_{ij}^{(new)} = Y_{ij} - \frac{Y_{ik} Y_{kj}}{Y_{kk}} \quad i, j = 1, 2, ..., n \qquad i, j \neq k \tag{6.4}$$

where $Y_{ij}^{(new)}$ is the equivalent ij element of the new Y-matrix.

To test the implemented function and show the difference of the equivalent matrix, a fault is applied on Bus 5 at *t = 1 sec*. Equation 6.5 represents the reduced pre-fault Y-matrix:

$Y^{prefault} =$

$$\begin{bmatrix}
2.1707 & 0.0930 & 0.0730 & -0.1025 & -0.0475 & -0.0270 & -0.0340 & -1.7530 & -0.5464 & 0.1805 \\
0.0930 & 0.4690 & 0.1557 & -0.1029 & -0.0475 & -0.0424 & -0.0391 & -0.2049 & -0.0945 & -0.1217 \\
0.0730 & 0.1557 & 0.7546 & -0.1468 & -0.0677 & -0.0630 & -0.0567 & -0.2431 & -0.1197 & -0.2040 \\
-0.1025 & -0.1029 & -0.1468 & 2.0075 & -0.6764 & -0.2245 & -0.1717 & -0.1732 & -0.1632 & -0.1585 \\
-0.0475 & -0.0475 & -0.0677 & -0.6764 & 1.2884 & -0.1043 & -0.0793 & -0.0793 & -0.0748 & -0.0726 \\
-0.0270 & -0.0424 & -0.0630 & -0.2245 & -0.1043 & 0.8615 & -0.0713 & -0.1217 & -0.1078 & -0.1122 \\
-0.0340 & -0.0391 & -0.0567 & -0.1717 & -0.0793 & -0.0713 & 0.6286 & -0.0824 & -0.0754 & -0.0756 \\
-1.7530 & -0.2049 & -0.2431 & -0.1732 & -0.0793 & -0.1217 & -0.0824 & 3.3447 & 0.1697 & -0.8577 \\
-0.5464 & -0.0945 & -0.1197 & -0.1632 & -0.0748 & -0.1078 & -0.0754 & 0.1697 & 1.2826 & -0.2911 \\
0.1805 & -0.1217 & -0.2040 & -0.1585 & -0.0726 & -0.1122 & -0.0756 & -0.8577 & -0.2911 & 1.5707
\end{bmatrix}$$

$+ j$

$$\begin{bmatrix}
-33.1117 & 2.5287 & 2.9219 & 2.1877 & 0.9928 & 2.2509 & 1.2736 & 11.3978 & 3.4914 & 7.6019 \\
2.5287 & -27.2187 & 10.1910 & 1.7675 & 0.8021 & 1.8193 & 1.0293 & 1.4829 & 0.9560 & 6.0180 \\
2.9219 & 10.1910 & -29.2739 & 2.4530 & 1.1132 & 2.5249 & 1.4284 & 1.7435 & 1.1984 & 5.1460 \\
2.1877 & 1.7675 & 2.4530 & -35.8053 & 15.6324 & 5.3579 & 3.0304 & 1.5684 & 1.6711 & 1.4147 \\
0.9928 & 0.8021 & 1.1132 & 15.6324 & -24.7596 & 2.4315 & 1.3752 & 0.7117 & 0.7583 & 0.6420 \\
2.2509 & 1.8193 & 2.5249 & 5.3579 & 2.4315 & -32.2626 & 14.3246 & 1.6173 & 1.7224 & 1.4588 \\
1.2736 & 1.0293 & 1.4284 & 3.0304 & 1.3752 & 14.3246 & -22.8891 & 0.9143 & 0.9739 & 0.8247 \\
11.3978 & 1.4829 & 1.7435 & 1.5684 & 0.7117 & 1.6173 & 0.9143 & -26.4205 & 4.2941 & 3.9329 \\
3.4914 & 0.9560 & 1.1984 & 1.6711 & 0.7583 & 1.7224 & 0.9739 & 4.2941 & -14.4206 & 1.4280 \\
7.6019 & 6.0180 & 5.1460 & 1.4147 & 0.6420 & 1.4588 & 0.8247 & 3.9329 & 1.4280 & -23.3890
\end{bmatrix} \quad (6.5)$$

After applying the fault on Bus 5, Equation 6.6 represent the reduced Y-matrix:

$Y^{fault} =$

$$\begin{bmatrix}
0.0000 & 0.0000 & 0.0000 & 0.0000 & 0.0000 & 0.0000 & 0.0000 & 0.0000 & 0.0000 & 0.0000 \\
0.0000 & 0.1733 & 0.0769 & -0.0063 & -0.0029 & -0.0014 & -0.0020 & -0.0101 & -0.0052 & 0.0085 \\
0.0000 & 0.0769 & 0.8301 & -0.0379 & -0.0177 & 0.0023 & -0.0086 & -0.0721 & -0.0356 & 0.0135 \\
0.0000 & -0.0063 & -0.0379 & 2.0425 & -0.6604 & -0.1942 & -0.1532 & -0.2037 & -0.1617 & -0.0455 \\
0.0000 & -0.0029 & -0.0177 & -0.6604 & 1.2956 & -0.0905 & -0.0709 & -0.0933 & -0.0742 & -0.0210 \\
0.0000 & -0.0014 & 0.0023 & -0.1942 & -0.0905 & 0.8867 & -0.0557 & -0.1397 & -0.1050 & -0.0150 \\
0.0000 & -0.0020 & -0.0086 & -0.1532 & -0.0709 & -0.0557 & 0.6383 & -0.0957 & -0.0741 & -0.0161 \\
0.0000 & -0.0101 & -0.0721 & -0.2037 & -0.0933 & -0.1397 & -0.0957 & 2.5101 & -0.0690 & -0.8352 \\
0.0000 & -0.0052 & -0.0356 & -0.1617 & -0.0742 & -0.1050 & -0.0741 & -0.0690 & 1.2180 & -0.2580 \\
0.0000 & 0.0085 & 0.0135 & -0.0455 & -0.0210 & -0.0150 & -0.0161 & -0.8352 & -0.2580 & 1.9404
\end{bmatrix}$$

$+j$

$$\begin{bmatrix}
0.0000 & 0.0000 & 0.0000 & 0.0000 & 0.0000 & 0.0000 & 0.0000 & 0.0000 & 0.0000 & 0.0000 \\
0.0000 & -37.5389 & 1.6368 & 0.1416 & 0.0643 & 0.1457 & 0.0824 & 0.1083 & 0.0669 & 0.5287 \\
0.0000 & 1.6368 & -36.3417 & 1.1512 & 0.5225 & 1.1839 & 0.6700 & 0.8813 & 0.5442 & 0.7522 \\
0.0000 & 0.1416 & 1.1512 & -35.9647 & 15.5601 & 5.1930 & 2.9373 & 1.9427 & 1.7065 & 0.8851 \\
0.0000 & 0.0643 & 0.5225 & 15.5601 & -24.7924 & 2.3567 & 1.3330 & 0.8816 & 0.7744 & 0.4017 \\
0.0000 & 0.1457 & 1.1839 & 5.1930 & 2.3567 & -32.4331 & 14.2283 & 2.0028 & 1.7587 & 0.9108 \\
0.0000 & 0.0824 & 0.6700 & 2.9373 & 1.3330 & 14.2283 & -22.9434 & 1.1323 & 0.9944 & 0.5153 \\
0.0000 & 0.1083 & 0.8813 & 1.9427 & 0.8816 & 2.0028 & 1.1323 & -23.0014 & 5.2421 & 5.2775 \\
0.0000 & 0.0669 & 0.5442 & 1.7065 & 0.7744 & 1.7587 & 0.9944 & 5.2421 & -14.1813 & 1.5710 \\
0.0000 & 0.5287 & 0.7522 & 0.8851 & 0.4017 & 0.9108 & 0.5153 & 5.2775 & 1.5710 & -25.1510
\end{bmatrix} \quad (6.6)$$

By applying the fault at Bus 35, we present the corresponding Reduced Y-matrix by Equation 6.7.

$Y^{fault} =$

$$\begin{bmatrix}
2.1707 & 0.0930 & 0.0730 & -0.1025 & -0.0475 & 0.0000 & -0.0340 & -1.7530 & -0.5464 & 0.1805 \\
0.0930 & 0.4690 & 0.1557 & -0.1029 & -0.0475 & 0.0000 & -0.0391 & -0.2049 & -0.0945 & -0.1217 \\
0.0730 & 0.1557 & 0.7546 & -0.1468 & -0.0677 & 0.0000 & -0.0567 & -0.2431 & -0.1197 & -0.2040 \\
-0.1025 & -0.1029 & -0.1468 & 2.0075 & -0.6764 & 0.0000 & -0.1717 & -0.1732 & -0.1632 & -0.1585 \\
-0.0475 & -0.0475 & -0.0677 & -0.6764 & 1.2884 & 0.0000 & -0.0793 & -0.0793 & -0.0748 & -0.0726 \\
0.0000 & 0.0000 & 0.0000 & 0.0000 & 0.0000 & 0.0000 & 0.0000 & 0.0000 & 0.0000 & 0.0000 \\
-0.0340 & -0.0391 & -0.0567 & -0.1717 & -0.0793 & 0.0000 & 0.6286 & -0.0824 & -0.0754 & -0.0756 \\
-1.7530 & -0.2049 & -0.2431 & -0.1732 & -0.0793 & 0.0000 & -0.0824 & 3.3447 & 0.1697 & -0.8577 \\
-0.5464 & -0.0945 & -0.1197 & -0.1632 & -0.0748 & 0.0000 & -0.0754 & 0.1697 & 1.2826 & -0.2911 \\
0.1805 & -0.1217 & -0.2040 & -0.1585 & -0.0726 & 0.0000 & -0.0756 & -0.8577 & -0.2911 & 1.5707
\end{bmatrix}$$

$+j$

$$\begin{bmatrix}
-33.1117 & 2.5287 & 2.9219 & 2.1877 & 0.9928 & 0.0000 & 1.2736 & 11.3978 & 3.4914 & 7.6019 \\
2.5287 & -27.2187 & 10.1910 & 1.7675 & 0.8021 & 0.0000 & 1.0293 & 1.4829 & 0.9560 & 6.0180 \\
2.9219 & 10.1910 & -29.2739 & 2.4530 & 1.1132 & 0.0000 & 1.4284 & 1.7435 & 1.1984 & 5.1460 \\
2.1877 & 1.7675 & 2.4530 & -35.8053 & 15.6324 & 0.0000 & 3.0304 & 1.5684 & 1.6711 & 1.4147 \\
0.9928 & 0.8021 & 1.1132 & 15.6324 & -24.7596 & 0.0000 & 1.3752 & 0.7117 & 0.7583 & 0.6420 \\
0.0000 & 0.0000 & 0.0000 & 0.0000 & 0.0000 & 0.0000 & 0.0000 & 0.0000 & 0.0000 & 0.0000 \\
1.2736 & 1.0293 & 1.4284 & 3.0304 & 1.3752 & 0.0000 & -22.8891 & 0.9143 & 0.9739 & 0.8247 \\
11.3978 & 1.4829 & 1.7435 & 1.5684 & 0.7117 & 0.0000 & 0.9143 & -26.4205 & 4.2941 & 3.9329 \\
3.4914 & 0.9560 & 1.1984 & 1.6711 & 0.7583 & 0.0000 & 0.9739 & 4.2941 & -14.4206 & 1.4280 \\
7.6019 & 6.0180 & 5.1460 & 1.4147 & 0.6420 & 0.0000 & 0.8247 & 3.9329 & 1.4280 & -23.3890
\end{bmatrix} \quad (6.7)$$

Notice that for the faulted matrix when the fault is applied on Bus 5, the most affected equivalent Bus is 1 because Bus 31 (Generator 2) is the closest electrically to Bus 5. However,

when the fault is applied on Bus 35, Generator 6 becomes off the network and therefore, Bus 6 of the equivalent network is the most affected since it is the closest electrically.

6.3.4 Determination of Severely Disturbed Groups (SDG):

As previously explained, for the proposed method to work, the system has to be separated into two groups: the severely disturbed machines group and the less disturbed machines group. To determine the SDG, the acceleration or accelerating power can be used to sort these groups. In this simulation, the SDG has to consist of at least two machines. The Table 6.1 is obtained to illustrate this method

Table 6.1: SDG Determination Illustration

Faulted Bus	Absolute Rotor Acceleration										Critical Machines
	1	2	3	4	5	6	7	8	9	10	
5	8.35	1.99	11.10	23.88	16.22	25.85	21.92	37.95	17.19	39.23	8,10
28	5.72	1.77	1.89	19.39	20.60	25.99	21.12	38.59	13.52	21.92	6,8
15	6.18	2.50	3.39	12.99	10.50	24.27	18.49	33.87	18.25	35.94	8,10
13	7.29	2.07	0.98	22.24	16.50	25.50	20.68	37.14	18.47	39.08	8,10
19	5.14	2.88	4.30	13.04	4.93	7.41	9.46	30.83	21.05	38.19	8,10
36	6.04	5.55	2.69	18.37	20.88	24.99	24.29	29.08	20.29	42.55	8,10
2	6.62	3.58	0.21	19.17	18.04	20.71	26.16	38.09	16.27	31.04	8,10
37	6.34	25.97	4.30	15.53	25.10	24.82	16.22	36.30	15.66	38.26	8,10

From Table 6.1, the critical groups of machines are determined using the absolute acceleration of each machine with a tolerance of 8. In most of the simulated cases, there are two severely disturbed machines. However, in some cases, the specified tolerance does not give at least two critical machines. Therefore, the generator with the second largest absolute acceleration is used to create the SDG. For example, when the fault is applied on Bus 28, the severely disturbed machine is generator 8, but there is not any generator that has an absolute acceleration within 8 p.u of generator 8's absolute acceleration, and therefore, generator 6 is added to the SDG. The same discussion applies to when the fault is applied to Bus 36. It can be noted that

machines 8 and 10 always swing together which indicates that these two machines are the ones that may cause instability.

6.3.5 TEF for COI Reference Frame with Classical Model

There are three direct methods to be applied in this section. The first method is based on [1]. Time-domain simulation is run up to the instant of fault clearing to obtain the angles and speeds of the generators. These values are used to calculate the total energy of the system at the fault clearing. After that, the critical energy V_{cr} is calculated using any appropriate method. The critical energy calculation is the most difficult step in applying the TEF method because it involves calculating the controlling UEP for the post-fault configuration. Due to the difficulty of calculating the UEP, the system's post-fault configuration is assumed to be the same as the pre-fault system's configuration which makes it easier to estimate the UEP from the power flow results ($UEP_i = \pi - SEP_i$). The criteria of this method is that if the system's total energy at the clearing instant for the post-fault configuration is greater than the critical energy, then the system is considered to be stable.

The second method is based on EEAC which is explained in Chapter 4. The method uses δ^0 and δ^s from the numerical simulation. Also, the Y-matrix is required as well as the steady-state generator's voltage. As previously explained, if the decelerating energy is greater than the accelerating energy, then the system is stable.

The third method is based on our proposal which involves calculating the individual machine potential and kinetic energies. In this method, the lowest potential energy of the post-fault configuration is compared with the largest kinetic energy of the fault clearing time. If the lowest potential energy is greater than the largest kinetic energy, then the system is stable.

Tables 6.2, 6.3, and 6.4 show the results of the three methods discussed previously compared to the numerical method. Also, the computational speed is considered for each method using a fixed time step of *1 ms*.

Table 6.2: Total Energy Comparison

Faulted Bus	t_c (*sec*)	t_{cr} (*sec*)	**Total Energy Comparison**			**Time-domain Assessment**
			V_{cr} = *286.3173*			
			V_{cl}	**Assess.**	**Sim. Time (*sec*)**	
5	0.27	0.25	289.9953	Unstable	23.703	Unstable
5	0.25		287.1471	Unstable	24.953	Stable
5	0.23		282.0698	Stable	23.656	Stable
28	0.18	0.17	282.5747	Stable	24.891	Unstable
28	0.17		282.6927	Stable	25.079	Stable
28	0.04		282.4158	Stable	25.594	Stable
15	0.27	0.27	287.0069	Unstable	25.797	Unstable
15	0.25		286.0387	Stable	29.125	Stable
13	0.28	0.27	286.8628	Unstable	29.469	Unstable
13	0.27		279.2869	Stable	25.938	Stable
19	0.22	0.20	286.7965	Unstable	25.281	Unstable
19	0.2		285.2112	Stable	25.438	Stable
36	0.27	0.25	288.2145	Unstable	25.563	Unstable
36	0.22		288.1847	Unstable	33.317	Stable
2	0.34	0.33	288.0676	Unstable	34.39	Unstable
2	0.25		283.9973	Stable	33.094	Stable
37	0.25	0.24	289.3173	Unstable	35.485	Unstable
37	0.23		286.0547	Stable	34.303	Stable

Table 6.3: EEAC Method

Faulted Bus	t_c (sec)	t_{cr} (sec)	Energy		Assess.	Sim. Time (sec)	Time-domain Assess.
			A_a	A_d			
5	0.27	0.25	10.529	7.2401	Unstable	23.406	Unstable
5	0.25		9.2765	8.9125	Unstable	24.657	Stable
5	0.23		8.0706	8.2397	Stable	24.141	Stable
28	0.18	0.17	-0.1569	8.7634	Failed	23.314	Unstable
28	0.04		-0.0147	8.1615	Failed	22.156	Stable
15	0.28	0.27	7.7641	7.6539	Unstable	23.297	Unstable
15	0.25		7.6213	8.9619	Stable	22.547	Stable
13	0.28	0.27	11.5682	10.6194	Unstable	21.984	Unstable
13	0.27		10.2936	11.2111	Stable	23.437	Stable
19	0.22	0.20	7.2164	6.7982	Unstable	25.641	Unstable
19	0.2		6.811	7.8988	Stable	23.062	Stable
36	0.27	0.25	-0.2417	7.2417	Failed	20.953	Unstable
36	0.22		-0.2109	7.1715	Failed	21.593	Stable
2	0.34	0.33	9.7575	9.1413	Unstable	22.937	Unstable
2	0.25		8.5481	8.8249	Stable	24.718	Stable
37	0.25	0.24	10.7707	10.4872	Unstable	21.187	Unstable
37	0.23		10.4479	11.0298	Stable	23.204	Stable

As seen in Tables 6.2 and 6.3, both methods result in very similar results. In fact, the EEAC is a part of the energy comparison since it uses the potential energy of the severely disturbed machine rather than the entire system. Also, it can be noted that the EEAC is faster than the total energy comparison especially that it focuses on one machine only unlike the total energy comparison method. However, the EEAC failed in some cases to produce the correct results because it gives negative energy in some case, e.g. faults on Bus 28 and Bus 36. Notice that in Table 6.2 when a fault is applied to Bus 28, the method failed to determine the system's stability correctly. Similarly, when a fault is applied to Bus 36, the energy comparison failed to determine the system's stability. Likewise, the EEAC failed to determine stability when a fault is applied to Bus 28 or Bus 36. Notice that the last row of each of the applied faults is considered to be the critical clearing status using the direct method tested in that particular table unless the method failed to assess stability correctly. For example, in Table 6.2, the critical clearing time

using total energy comparison method is 0.23 sec when a fault is applied to Bus 5. Similar example from Table 6.3 is that the critical clearing time using EEAC is 0.25 seconds when a fault is applied to Bus 15. Also, the energy conversion nature of the TEF methods can be noted in Table 6.3 where the sum of accelerating and decelerating energies is approximately constant regardless of varying the fault clearing time. Additionally, the transient stability assessment is conservative as seen from both Table 6.2 and Table 6.3.

Table 6.4 shows results of the proposed method simulation results.

Table 6.4: Proposed Method Simulation for COI Reference Frame

Faulted Bus	Fault Clearing Time (sec)	Critical Clearing Time (sec)	No. of Critical Machines	Single-Machine Energy		Assess.	Time-domain Assess.	Sim. Time (sec)	TD Sim. Time (sec)
				KE_{max}	PE_{min}				
5	0.27	0.25	2	9.5205	7.4946	Unstable	Unstable	25.016	113.235
5	0.25		2	8.4549	8.4241	Unstable	Stable	24.167	109.967
5	0.23		2	7.3563	7.4413	Stable	Stable	24.141	109.703
28	0.18	0.17	2	4.7734	4.3945	Unstable	Stable	23.188	143.042
28	0.15		2	3.6722	4.3400	Stable	Stable	22.656	209.394
15	0.28	0.27	2	7.3617	7.2912	Unstable	Unstable	23.297	108.582
15	0.25		2	6.5705	7.2339	Stable	Stable	23.453	108.296
13	0.28	0.27	2	9.1216	7.3227	Unstable	Unstable	22.922	114.343
13	0.27		2	8.1699	7.2715	Unstable	Stable	23.89	113.332
13	0.23		2	6.3996	7.1760	Stable	Stable	23.25	108.375
19	0.22	0.20	2	9.0789	6.3822	Unstable	Unstable	23.672	115.604
19	0.2		2	7.7569	6.4464	Unstable	Stable	23.812	113.937
19	0.18		2	6.5064	6.5352	Stable	Stable	23.0313	111.521
36	0.27	0.25	2	7.9451	6.2371	Unstable	Unstable	22.275	115.914
36	0.25		2	7.0351	6.2969	Unstable	Stable	23.219	114.893
36	0.23		2	6.1752	6.3553	Stable	Stable	21.781	113.274
2	0.35	0.33	2	8.2834	8.1943	Unstable	Unstable	21.841	114.963
2	0.32		2	6.5097	9.9698	Stable	Stable	22.573	115.583
37	0.25	0.24	2	7.0505	6.5332	Unstable	Unstable	21.187	114.185
37	0.22		2	5.3745	5.4385	Stable	Stable	22.609	111.070

From Table 6.4, the proposed method works as good as the total energy comparison method and EEAC method. Also, the average simulation time of this method is less than that of the other two methods. Notice that the proposed method works only if sectors of severely

disturbed machines are formed depending on the accelerating power. A tolerance of 8 pu in the absolute acceleration is used to make sectors of severely disturbed machines. This tolerance is chosen to be 20% of the largest absolute acceleration. The percentage is found using the ratio of the largest absolute acceleration to the total absolute acceleration. This tolerance is chosen to be 8 pu exactly because experimenting with the particular test system shows that it was a good choice. For different systems, the tolerance may be chosen differently. Some improvement is required in order to make the method work for any small or large power system. Notice that the last row of each fault trial is considered to be the critical status. For example, as in Table 6.4, when a fault is applied to Bus 36, the critical clearing time using the proposed method is 0.23 seconds. Similarly, the critical clearing time using the proposed method is 0.18 seconds if a fault is applied to Bus 19.

Table 6.5 shows the average simulation time for the three methods for the different faults applied previously. Also, the numerical method simulation time for 4 seconds is compared with the other three methods.

Table 6.5: Average Simulation Time

Faulted Bus	Method			
	Energy Comparison	EEAC	Proposed Method	Numerical Integration (Forward Euler)
	Average Simulation Time (sec)			
5	24.1040	24.0680	24.4413	110.9683
28	25.1880	23.1057	22.9220	176.2180
15	27.4610	22.9220	23.3750	108.4390
13	27.7035	22.7105	23.3540	112.0167
19	25.3595	24.3515	23.5051	113.6873
36	29.4402	21.2730	21.9657	114.5940
2	33.7420	23.8275	22.1810	114.2730
37	34.8940	22.1955	21.8980	112.1275

From Table 6.5, the energy comparison method is slower than both the EEAC and the proposed method. However, the three different TEF methods are far more superior in simulation time than the numerical methods, which is the main advantage of using TEF methods. Note that there is some additional numerical integration time added. In average, the calculation of the energy function requires less than 3 seconds to complete and determine stability.

In Table 6.6, the procedure explained in the flow chart of Figure 6.1 is used to determine the critical clearing time for different fault locations.

Table 6.6: Determining Critical Clearing Time Using Proposed Method

Faulted Bus	t_{cr} *(sec)* (numerical methods)	t_{cr} *(sec)* (proposed method)	Number of Iterations	Simulation Time (*sec*)
5	0.250	0.23164	26	296.766
28	0.167	0.15853	44	448.187
15	0.267	0.26517	18	197.875
13	0.267	0.24902	15	148.156
19	0.200	0.18288	16	126.547
36	0.250	0.23649	13	109.844
2	0.333	0.32884	12	119.375
37	0.242	0.21986	40	446.516

From Table 6.6, it can be seen that the proposed method gives conservative critical clearing time. Although the search technique takes considerably many iterations, it still is faster than numerical methods which may require a simulation of 10 seconds or more to determine the transient stability. Additionally, the proposed method is considerably more accurate than the total energy comparison method and the EEAC method tested in this thesis which is shown in Table 6.7.

Table 6.7: Comparison of the Four Methods in determining t_{cr}

Faulted Bus	t_{cr} *(sec)* (numerical methods)	t_{cr} *(sec)* (Total energy comparison)	t_{cr} *(sec)* (EEAC)	t_{cr} *(sec)* (proposed method)
5	0.250	0.233	0.233	0.23164
28	0.167	Failed	Failed	0.15853
15	0.267	0.250	0.250	0.26517
13	0.267	0.267	0.267	0.24902
19	0.200	0.200	0.200	0.18288
36	0.250	Failed	Failed	0.23649
2	0.333	0.250	0.250	0.32884
37	0.242	0.233	0.233	0.21986

From Table 6.7, the proposed method is fairly more accurate than the total energy comparison method and the EEAC method.

In Section 6.3.6, the proposed method is applied using the synchronous reference frame model.

6.3.6 TEF for Synchronous Reference Frame with Classical Model

In this section, the proposed method is used to determine stability using synchronous reference frame. This method is based on the individual machine potential and kinetic energy. If the post-fault potential energy is greater than the kinetic energy at the clearing time, then the system is stable. Note that for this method to work, sectors of critical machines has to be formed using the same principle of accelerating energy (total power of individual machines at fault occurrence $t = 0^+$). This method uses Equations 4.10 and 4.13 to perform the proposed method.

Table 6.8 shows the proposed method applied for synchronous reference frame.

Table 6.8: Proposed Method Simulation for Synchronous Reference Frame

Faulted Bus	Fault Clearing Time (sec)	Critical Clearing Time (sec)	No. of Critical Machines	Single-Machine Energy		Assess.	Time-domain Assess.	Sim. Time (sec)	TD Sim. Time (sec)
				KE_{max}	PE_{min}				
5	0.30	0.28	2	15.6083	12.6267	Unstable	Unstable	24.608	84.859
5	0.28		2	14.1180	14.8807	Stable	Stable	22.953	82.093
28	0.20	0.18	2	9.1752	7.8321	Unstable	Unstable	21.891	85.549
28	0.18		2	6.6581	12.5076	Stable	Stable	22.625	83.735
15	0.28	0.27	2	14.4091	8.2736	Unstable	Unstable	26.853	81.783
15	0.27		2	13.0236	13.6986	Stable	Stable	23.159	85.890
13	0.32	0.30	2	16.3764	14.0813	Unstable	Unstable	29.938	84.095
13	0.30		2	14.9446	16.7450	Stable	Stable	26.610	82.859
19	0.23	0.22	2	13.4026	13.2719	Unstable	Unstable	23.328	89.857
19	0.22		2	11.6791	12.6948	Stable	Stable	24.844	87.185
36	0.33	0.32	2	17.6708	15.3340	Unstable	Unstable	26.468	91.659
36	0.32		2	16.0545	17.0974	Stable	Stable	27.234	82.589
2	0.32	0.30	2	14.8570	8.6873	Unstable	Unstable	29.391	84.951
2	0.30		2	13.5089	10.1705	Unstable	Stable	28.453	82.589
2	0.28		2	12.2115	14.8831	Stable	Stable	28.203	81.573
37	0.27	0.25	2	11.9685	7.0611	Unstable	Unstable	26.078	84.379
37	0.25		2	10.6008	8.3389	Unstable	Stable	28.609	79.789
37	0.23		2	9.3091	9.3927	Stable	Stable	28.859	80.853

From Table 6.8, the proposed method gives fairly consistent results compared to the numerical integration method. The critical clearing time from the proposed method is very close to the critical clearing of the numerical integration. There is not any failed attempt with the proposed method determining whether the system is stable or unstable. Also, the conservative nature of energy functions can clearly be noticed. That is, the critical clearing time using the proposed method is always less than the actual one.

Table 6.9 shows the average simulation time of the proposed method as well as the numerical integration method for 4 seconds.

Table 6.9: Average Simulation Time

Faulted Bus	Method	
	Proposed Method	Numerical Integration (Forward Euler)
	Simulation Time (sec)	
5	23.781	83.476
28	22.258	84.642
15	25.006	83.837
13	28.274	83.477
19	24.086	88.521
36	26.851	87.124
2	28.682	83.038
37	27.849	81.674

From Table 6.9, the EEAC and the proposed method have fast simulating time compared to the numerical integration method. That shows the suitability of TEF methods for operation purposes unlike the numerical integration which is suitable for planning purposes only.

6.4 Summary:

In this chapter, an algorithm for the proposed method is presented and used to perform the simulation. PSAT package is introduced and some of its features are tested. PSAT includes power flow calculations and time-domain integration which are the needed tools for this thesis. Also, three direct methods in the COI reference frame are simulated on the IEEE 39 Bus power system using PSAT and MATLAB. The three direct methods are based on TEF: total energy comparison to the critical potential energy, the EEAC, and the proposed method which is based on single-machine TEF. The three methods are compared with the numerical integration which is used as a benchmark for this thesis. In addition, the proposed method is simulated in the synchronous reference frame and the results are compared with the numerical integration method.

Concluding remarks and suggestions for future work for this thesis are presented in Chapter 7.

CHAPTER 7

CONCLUDING REMARKS AND FUTURE WORK

7.1 Concluding Remarks:

The research demonstrated in the thesis provides an alternative direct method to assess transient stability of a multi-machine power system. The proposed method is based on transient energy function methods, which can be used to determine transient stability directly without solving the power system equations numerically. It uses the energy conversion phenomena for any object. The method basically uses the single machine smallest post-fault potential and largest fault clearing kinetic energies which are compared with each other. If the potential energy is greater than the kinetic energy, then the system is considered stable. However, since the system may have more than one machine that is severely disturbed, the energies are sorted in order to group them so that the total kinetic energy of the severely disturbed group is compared with the group of machines that have the lowest post-fault potential energy.

The proposed method is applied on the IEEE 39 Bus power system for several fault cases. The method performance is verified by comparing it with the numerical methods results. The method produces a conservative result which is as expected for any direct method. For now, the proposed method is an effective tool for planning purposes, which is faster than the numerical integration that is dependent on the integration step size. For example, the proposed method can be used in the "what-if" scenarios which may require very long time if numerical integration is used.

Also, the proposed method is compared with other direct methods such as, EEAC and critical energy comparison, and numerical methods such as, forward Euler numerical integration. The proposed method is shown to be very effective to assess transient stability.

The simulation time of the proposed method is also compared with the numerical integration method as well as with the EEAC and critical energy comparison. It is shown that the proposed method has improved speed if compared with the other direct methods. It is also shown that the proposed method is much faster than the numerical integration method. Note that the proposed method requires numerical integration up to the clearing instant which is an advantage over the numerical integration methods.

A historical review of stability analysis is presented in this thesis. The stability analysis is classified into two classes: small-signal stability and transient stability. The focal point of this thesis is transient stability analysis. Transient stability analysis methods are presented in this thesis. There are two main methods of transient stability analysis: numerical methods and direct methods. Different numerical methods are discussed in this thesis such as, trapezoidal rule and Euler integration. Additionally, different methods of direct methods are presented, and the advantages and disadvantages of these methods over numerical methods are discussed.

The tool to test the proposed method is a MATLAB based toolbox titled Power System Analysis Toolbox (PSAT). PSAT is used for electric power system analysis and control. PSAT is used in this thesis because of its availability and capability of performing power flow and numerical integration in addition to its easy-to-use graphical user interface (GUI) as well as its capability of command usage.

7.2 Future Work:

For future work, the proposed method can be improved by using a better searching method of severely disturbed machines. Also, the method can be tested for a different post-fault configuration which may require some optimization techniques since the post-fault trajectories are unknown. In addition, the code can be optimized to perform the analysis faster than it is now. A better program may improve the analysis such as, EMTP-RV. Detailed model for direct methods for transient stability analysis is still being investigated and can be included in future work. Additionally, the proposed method can be improved to be used for operational decisions at which fast decisions are required.

APPENDIX A

A.1 Software Development:

In this section of the thesis, we explain the coding techniques used to implement the three methods described in Chapter 4. The code is written in MATLAB R2008b. The three methods start with the following set of implementation:

- Load system file (ieee39bus.m)
- Set up PSAT: - Use forward Euler numerical integration
  - Use COI
  - Use time step of 10^{-3} seconds
  - Set the end time to be the same as the fault clearing time
- Run power flow
- Start time counter
- Run time-domain numerical integration up to the fault clearing instant
- Record the resulted rotor angles and rotor speeds of the fault clearing instant
- Use KronR.m to reduce the Y-matrix to be 10×10 for the during-fault and post-fault settings

Now, the three methods can be applied. The first method, the total energy comparison, is implemented as follows:

- Use sum(KE.m) to calculate the total kinetic energy
- Use sum(PE.m) to calculate the total potential energy and the critical energy
- Determine stability by comparing the sum of energy with the critical energy
- Stop the counter

The second method, EEAC, is implemented as follows:

- Determine the SDM using SDM.m
- Use Aa.m to determine accelerating energy
- Calculate the UEP
- Use Ad.m to determine decelerating energy
- Determine stability using explanations in chapter 4
- Stop counter

The third method, the proposed one, is implemented as follows:

- Use SDG.m to calculate the absolute acceleration of each generator
- Use KE.m to calculate the kinetic energy of each generator
- Use PE.m to calculate the potential energy of each generator
- Determine stability using the criterion explained in chapter 4
- Stop counter

The functions KE.m, PE.m, Aa, Ad, SDM.m, and SDG.m are implementations of the equations explained in details in chapter 4.

A.2 PSAT Built-in Functions [22]:

Some important built-in PSAT functions are used to implement the data file, faults, and running required analyses. At first, PSAT data format is explained for the components used in this thesis.

A.2.1 Bus Data Format:

Table A.2.1 shows the Bus data format using the command `Bus.con`.

Table A.2.1: Bus Data Format (`Bus.con`)

Coulmn	Variable	Description	Unit
1	-	Bus number	int
2	V_s	Voltage base	kV
3	V_0	Voltage amplitude initial guess	p.u.
4	θ_0	Voltage phase initial guess	rad

A.2.2 Line Data Format:

Table A.2.2 shows the line data format in PSAT using the command (`Line.con`).

Table A.2.2: Line Data Format (`Line.con`)

Column	Variable	Decription	Unit
1	k	From Bus	int
2	m	To Bus	int
3	S_n	Power rating	MVA
4	V_n	Voltage rating	kV
5	f_n	Frequency rating	Hz
6	l	Line length	km
7	-	not used	-
8	r	Resistance	p.u. (Ω/km)
9	x	Reactance	p.u. (H/km)
10	b	Suscptance	p.u. (F/km)
11	-	not used	-
12	-	not used	-
13	I_{max}	Current limit	p.u.
14	P_{max}	Active power limit	p.u.
15	S_{max}	Apparent power limit	p.u.
16	u	Connection status	{0,1}

A.2.3 Transformer Data Format:

Table A.2.3 shows the transformer data format in PSAT using the command (`Line.con`).

Table A.2.3: Transformer Data Format (`Line.con`)

Column	Variable	Decription	Unit
1	k	From Bus	int
2	m	To Bus	int
3	S_n	Power rating	MVA
4	V_n	Voltage rating	kV
5	f_n	Frequency rating	Hz
6	-	not used	-
7	K_T	Primary and secondary voltage ration	kV/kV
8	r	Resistance	p.u. (Ω/km)
9	x	Reactance	p.u. (H/km)
10	-	not used	-
11	a	Fixed tap ratio	p.u./p.u.
12	ϕ	Fixed phase shift	deg
13	I_{max}	Current limit	p.u.
14	P_{max}	Active power limit	p.u.
15	S_{max}	Apparent power limit	p.u.
16	u	Connection status	{0,1}

A.2.4 Slack Generator Data Format:

Table A.2.4 shows the slack generator data format in PSAT using the command (`SW.con`).

Table A.2.4: Slack Generator Data Format (`SW.con`)

Column	Variable	Description	Unit
1	-	Bus numer	int
2	S_n	Power rating	MVA
3	V_n	Voltage rating	kV
4	V_0	Voltage magnitude	p.u.
5	θ_0	Reference angle	p.u.
6	Q_{max}	Maximum reactive power	p.u.
7	Q_{min}	Minimum reactive power	p.u.
8	V_{max}	Maximum voltage	p.u.
9	V_{min}	Minimum voltage	p.u.
10	P_{g0}	Active power guess	p.u.
11	γ	Loss participation coefficient	-
12	z	Reference bus	{0,1}
13	u	Connection status	{0,1}

A.2.5 PV Generator Data Format:

Table A.2.5 shows the PV generator data format in PSAT using the command (`PV.con`).

Table A.2.5: PV Generator Data Format (`PV.con`)

Column	Variable	Description	Unit
1	-	Bus numer	int
2	S_n	Power rating	MVA
3	V_n	Voltage rating	kV
4	V_0	Voltage magnitude	p.u.
5	θ_0	Reference angle	p.u.
6	Q_{max}	Maximum reactive power	p.u.
7	Q_{min}	Minimum reactive power	p.u.
8	V_{max}	Maximum voltage	p.u.
9	V_{min}	Minimum voltage	p.u.
10	P_{g0}	Active power guess	p.u.
11	γ	Loss participation coefficient	-

A.2.6 PQ Load Data Format:

Table A.2.6 shows the PQ Load data format in PSAT using the command (`PQ.con`).

Table A.2.6: PQ Load Data Format (`PQ.con`)

Column	Variable	Description	Unit
1	-	Bus numer	int
2	S_n	Power rating	MVA
3	V_n	Voltage rating	kV
4	P_L	Active Power	p.u.
5	Q_L	Reactive Power	p.u.
6	V_{max}	Maximum Voltage	p.u.
7	V_{min}	Minimum Voltage	p.u.
8	z	Allow conversion to impedance	{0,1}
9	u	Connection status	{0,1}

A.2.7 Fault Data Format:

Table A.2.7 shows the fault data format in PSAT using the command (`Fault.con`).

Table A.2.7: Fault Data Format (`Fault.con`)

Column	Variable	Description	Unit
1	-	Bus numer	int
2	S_n	Power rating	MVA
3	V_n	Voltage rating	kV
4	f_n	Frequency rating	Hz
5	t_f	Fault time	S
6	t_c	Clearance time	s
7	r_f	Fault resistance	p.u.
8	x_f	Fault reactance	p.u.

A.2.8 Synchronous Machine Data Format:

Table A.2.8 shows the synchronous machine data format in PSAT using the command (`syn.con`).

Table A.2.8: Synchronous machine data format

Column	Variable	Description	Unit
1	-	Bus number	int
2	*Sn*	Power rating	MVA
3	*Vn*	Voltage rating	kV
4	*fn*	Frequency rating	Hz
5	-	Machine model	-
6	*xl*	Leakage reactance	p.u.
7	*ra*	Armature resistance	p.u.
8	*xd*	d-axis synchronous reactance	p.u.
9	*x'd*	d-axis transient reactance	p.u.
10	*x''d*	d-axis subtransient reactance	p.u.
11	*T'd0*	d-axis open circuit transient time constant	s
12	*T''d0*	d-axis open circuit subtransient time constant	s
13	*xq*	q-axis synchronous reactance	p.u.
14	*x'q*	q-axis transient reactance	p.u.
15	*x''q*	q-axis subtransient reactance	p.u.
16	*T'q0*	q-axis open circuit transient time constant	s
17	*T''q0*	q-axis open circuit subtransient time constant	s
18	*M = 2H*	Mechanical starting time	kWs/kVA
19	*D*	Damping coefficient	-
20	$K\omega$	Speed feedback gain	gain
21	*Kp*	Active power feedback gain	gain
22	γP	Active power ratio at node	[0,1]
23	γQ	Reactive power at node	[0,1]
24	*TAA*	d-axis additional leakage time constant	s
25	*S(1,0)*	First saturation factor	-
26	*S(1,2)*	second saturation factor	-
27	*nCOI*	Center of inertia number	int
28	*u*	Connection status	{0,1}

Notice that not all parameters are used when the classical model is used. Column 5 indicates the machine model and the number "2" indicates the classical model. For more details, refer to [22].

A.3 Power Flow Report:

POWER FLOW REPORT

P S A T 2.1.6

Author: Federico Milano, (c) 2002-2010
e-mail: Federico.Milano@uclm.es
website: http://www.uclm.es/area/gsee/Web/Federico

File: C:\Documents and Settings\Hussain\My Documents\Thesis Simulation\Using PSAT\ieee39bus3
Date: 26-Feb-2011 00:54:27

NETWORK STATISTICS

Buses: 39
Lines: 34
Transformers: 12
Generators: 10
Loads: 30

SOLUTION STATISTICS

Number of Iterations: 4
Maximum P mismatch [p.u.] 0
Maximum Q mismatch [p.u.] 0
Power rate [MVA] 100

POWER FLOW RESULTS

Bus	V [p.u.]	phase [rad]	P gen [p.u.]	Q gen [p.u.]	P load [p.u.]	Q load [p.u.]
Bus 01	1.059	-0.14526	0	0	0	0
Bus 02	1.0789	-0.10241	0	0	0	0
Bus 03	1.0696	-0.14979	0	0	3.22	0.024
Bus 04	1.053	-0.16671	0	0	5	1.84
Bus 05	1.0566	-0.15128	0	0	0	0
Bus 06	1.0602	-0.14094	0	0	0	0
Bus 07	1.0467	-0.17517	0	0	2.338	0.84
Bus 08	1.0441	-0.18286	0	0	5.22	1.76
Bus 09	1.048	-0.17709	0	0	0	0
Bus 10	1.0727	-0.10145	0	0	0	0
Bus 11	1.0673	-0.11485	0	0	0	0
Bus 12	1.0623	-0.11435	0	0	0.085	0.88
Bus 13	1.0687	-0.11182	0	0	0	0
Bus 14	1.0629	-0.13596	0	0	0	0

Bus 15	1.0625	-0.13658	0	0	3.2	1.53
Bus 16	1.0762	-0.11149	0	0	3.29	0.323
Bus 17	1.0755	-0.12912	0	0	0	0
Bus 18	1.0721	-0.1439	0	0	1.58	0.3
Bus 19	1.1115	-0.03129	0	0	0	0
Bus 20	0.99422	-0.0488	0	0	6.28	1.03
Bus 21	1.0691	-0.07211	0	0	2.74	1.15
Bus 22	1.0788	0.00133	0	0	0	0
Bus 23	1.0699	-0.00166	0	0	2.475	0.846
Bus 24	1.0789	-0.10948	0	0	3.086	-0.922
Bus 25	1.0877	-0.0797	0	0	2.24	0.472
Bus 26	1.0873	-0.09945	0	0	1.39	0.17
Bus 27	1.0765	-0.13189	0	0	2.81	0.755
Bus 28	1.0821	-0.04162	0	0	2.06	0.276
Bus 29	1.0803	0.00394	0	0	2.835	0.269
Bus 30	1.0475	-0.06033	2.5	1.2421	0	0
Bus 31	0.982	0	5.1092	2.5614	0	0
Bus 32	0.9831	0.04016	6.5	2.7299	0	0
Bus 33	0.9972	0.06022	6.32	1.8232	0	0
Bus 34	1.0123	0.04202	5.08	1.9822	0	0
Bus 35	1.0493	0.08771	6.5	1.9311	0	0
Bus 36	1.0635	0.1326	5.6	0.02211	0	0
Bus 37	1.0278	0.03839	5.4	-0.15336	0	0
Bus 38	1.0265	0.12695	8.3	-0.02723	0	0
Bus 39	1.03	-0.17221	10	-0.41522	11.04	2.5

STATE VARIABLES

delta_Syn_1	-0.11558
omega_Syn_1	1
delta_Syn_2	0.30206
omega_Syn_2	1
delta_Syn_3	0.34126
omega_Syn_3	1
delta_Syn_4	0.31139
omega_Syn_4	1
delta_Syn_5	0.52254
omega_Syn_5	1
delta_Syn_6	0.3527
omega_Syn_6	1
delta_Syn_7	0.37039
omega_Syn_7	1
delta_Syn_8	0.32415
omega_Syn_8	1
delta_Syn_9	0.54951
omega_Syn_9	1
delta_Syn_10	0.0078
omega_Syn_10	1

OTHER ALGEBRAIC VARIABLES

vf_Syn_1	1.0292
pm_Syn_1	10
p_Syn_1	10
q_Syn_1	-0.41522
vf_Syn_2	1.219

pm_Syn_2	5.1092
p_Syn_2	5.1092
q_Syn_2	2.5614
vf_Syn_3	1.1838
pm_Syn_3	6.5
p_Syn_3	6.5
q_Syn_3	2.7299
vf_Syn_4	1.1118
pm_Syn_4	6.32
p_Syn_4	6.32
q_Syn_4	1.8232
vf_Syn_5	1.4331
pm_Syn_5	5.08
p_Syn_5	5.08
q_Syn_5	1.9822
vf_Syn_6	1.1826
pm_Syn_6	6.5
p_Syn_6	6.5
q_Syn_6	1.9311
vf_Syn_7	1.0953
pm_Syn_7	5.6
p_Syn_7	5.6
q_Syn_7	0.02211
vf_Syn_8	1.0624
pm_Syn_8	5.4
p_Syn_8	5.4
q_Syn_8	-0.15336
vf_Syn_9	1.1238
pm_Syn_9	8.3
p_Syn_9	8.3
q_Syn_9	-0.02723
vf_Syn_10	1.0868
pm_Syn_10	2.5
p_Syn_10	2.5
q_Syn_10	1.2421
delta_COI_1	0.04508
omega_COI_1	1

LINE FLOWS

From Bus	To Bus	Line	P Flow [p.u.]	Q Flow [p.u.]	P Loss [p.u.]	Q Loss [p.u.]
Bus 01	Bus 02	1	-1.2236	-0.7754	0.00513	-0.73822
Bus 01	Bus 39	2	1.2236	0.7754	0.00261	-0.75315
Bus 02	Bus 03	3	3.6577	0.28743	0.01515	-0.12081
Bus 02	Bus 25	4	-2.3864	0.78892	0.03884	-0.12363
Bus 02	Bus 30	5	-2.5	-1.1135	0	0.12855
Bus 03	Bus 04	6	0.94264	0.65883	0.00171	-0.22136
Bus 03	Bus 18	7	-0.52006	-0.27459	0.00028	-0.24175
Bus 04	Bus 05	8	-1.3542	-0.28067	0.00135	-0.12765
Bus 04	Bus 14	9	-2.7049	-0.67914	0.00554	-0.06533
Bus 05	Bus 08	10	3.1821	0.92491	0.00798	-0.05109
Bus 06	Bus 05	11	4.5415	1.0799	0.00389	0.00192
Bus 06	Bus 07	12	4.2154	1.2794	0.01045	0.03481
Bus 06	Bus 11	13	-3.6477	-0.64462	0.00849	-0.05775

Bus 07	Bus 08	14	1.8669	0.40454	0.00135	-0.06977
Bus 08	Bus 09	15	-0.18032	-0.30968	9e-005	-0.41482
Bus 09	Bus 39	16	-0.18041	0.10513	0.00056	-1.2816
Bus 10	Bus 11	17	3.6643	0.98949	0.00504	-0.02931
Bus 10	Bus 13	18	2.8357	0.71192	0.00299	-0.0514
Bus 10	Bus 32	19	-6.5	-1.7014	0	1.0285
Bus 12	Bus 11	20	-0.00289	-0.42481	0.00026	0.00712
Bus 12	Bus 13	21	-0.08211	-0.45519	0.00031	0.00845
Bus 13	Bus 14	22	2.7503	0.29968	0.00609	-0.12743
Bus 14	Bus 15	23	0.03372	-0.18669	0	-0.41329
Bus 15	Bus 16	24	-3.1663	-1.3034	0.00915	-0.09991
Bus 16	Bus 17	25	2.286	-0.16084	0.00316	-0.11511
Bus 16	Bus 19	26	-5.0249	-1.5199	0.03738	0.09173
Bus 16	Bus 21	27	-3.3066	0.67473	0.00802	-0.15782
Bus 16	Bus 24	28	-0.42	-0.52046	0.00011	-0.07687
Bus 17	Bus 18	29	2.1031	0.21271	0.00273	-0.12014
Bus 17	Bus 27	30	0.17981	-0.25843	4e-005	-0.37177
Bus 19	Bus 33	31	-6.2895	-1.2054	0.03046	0.61784
Bus 19	Bus 20	32	1.2273	-0.40629	0.0012	0.02357
Bus 20	Bus 34	33	-5.0539	-1.4599	0.02612	0.52231
Bus 21	Bus 22	34	-6.0546	-0.31745	0.02568	0.15352
Bus 22	Bus 23	35	0.41968	0.86294	0.00058	-0.20386
Bus 22	Bus 35	36	-6.5	-1.3339	0	0.59717
Bus 23	Bus 24	37	3.5302	-0.51128	0.02413	-0.03286
Bus 23	Bus 36	38	-5.5861	0.73207	0.01386	0.75418
Bus 25	Bus 26	39	0.71814	-0.35373	0.0014	-0.59259
Bus 25	Bus 37	40	-5.3834	0.79429	0.01658	0.64093
Bus 26	Bus 27	41	2.6389	0.45217	0.00866	-0.18949
Bus 26	Bus 28	42	-1.4086	-0.17178	0.00752	-0.83507
Bus 26	Bus 29	43	-1.9035	-0.21153	0.01823	-1.0088
Bus 28	Bus 29	44	-3.4761	0.38729	0.01479	-0.13157
Bus 29	Bus 38	45	-8.2477	1.0472	0.0523	1.0199
Bus 06	Bus 31	46	-5.1092	-1.7146	0	0.84683

LINE FLOWS

From Bus	To Bus	Line	P Flow [p.u.]	Q Flow [p.u.]	P Loss [p.u.]	Q Loss
Bus 02	Bus 01	1	1.2287	0.03718	0.00513	-0.73822
Bus 39	Bus 01	2	-1.221	-1.5285	0.00261	-0.75315
Bus 03	Bus 02	3	-3.6426	-0.40824	0.01515	-0.12081
Bus 25	Bus 02	4	2.4253	-0.91256	0.03884	-0.12363
Bus 30	Bus 02	5	2.5	1.2421	0	0.12855
Bus 04	Bus 03	6	-0.94092	-0.88019	0.00171	-0.22136
Bus 18	Bus 03	7	0.52034	0.03284	0.00028	-0.24175
Bus 05	Bus 04	8	1.3555	0.15302	0.00135	-0.12765
Bus 14	Bus 04	9	2.7105	0.6138	0.00554	-0.06533
Bus 08	Bus 05	10	-3.1741	-0.976	0.00798	-0.05109
Bus 05	Bus 06	11	-4.5376	-1.0779	0.00389	0.00192
Bus 07	Bus 06	12	-4.2049	-1.2445	0.01045	0.03481
Bus 11	Bus 06	13	3.6561	0.58687	0.00849	-0.05775
Bus 08	Bus 07	14	-1.8656	-0.47431	0.00135	-0.06977
Bus 09	Bus 08	15	0.18041	-0.10513	9e-005	-0.41482
Bus 39	Bus 09	16	0.18098	-1.3867	0.00056	-1.2816
Bus 11	Bus 10	17	-3.6593	-1.0188	0.00504	-0.02931

Bus 13	Bus 10	18	-2.8327	-0.76332	0.00299	-0.0514
Bus 32	Bus 10	19	6.5	2.7299	0	1.0285
Bus 11	Bus 12	20	0.00316	0.43193	0.00026	0.00712
Bus 13	Bus 12	21	0.08242	0.46364	0.00031	0.00845
Bus 14	Bus 13	22	-2.7442	-0.42711	0.00609	-0.12743
Bus 15	Bus 14	23	-0.03372	-0.2266	0	-0.41329
Bus 16	Bus 15	24	3.1754	1.2035	0.00915	-0.09991
Bus 17	Bus 16	25	-2.2829	0.04573	0.00316	-0.11511
Bus 19	Bus 16	26	5.0622	1.6117	0.03738	0.09173
Bus 21	Bus 16	27	3.3146	-0.83255	0.00802	-0.15782
Bus 24	Bus 16	28	0.42011	0.44359	0.00011	-0.07687
Bus 18	Bus 17	29	-2.1003	-0.33284	0.00273	-0.12014
Bus 27	Bus 17	30	-0.17977	-0.11334	4e-005	-0.37177
Bus 33	Bus 19	31	6.32	1.8232	0.03046	0.61784
Bus 20	Bus 19	32	-1.2261	0.42986	0.0012	0.02357
Bus 34	Bus 20	33	5.08	1.9822	0.02612	0.52231
Bus 22	Bus 21	34	6.0803	0.47096	0.02568	0.15352
Bus 23	Bus 22	35	-0.4191	-1.0668	0.00058	-0.20386
Bus 35	Bus 22	36	6.5	1.9311	0	0.59717
Bus 24	Bus 23	37	-3.5061	0.47841	0.02413	-0.03286
Bus 36	Bus 23	38	5.6	0.02211	0.01386	0.75418
Bus 26	Bus 25	39	-0.71674	-0.23886	0.0014	-0.59259
Bus 37	Bus 25	40	5.4	-0.15336	0.01658	0.64093
Bus 27	Bus 26	41	-2.6302	-0.64166	0.00866	-0.18949
Bus 28	Bus 26	42	1.4161	-0.66329	0.00752	-0.83507
Bus 29	Bus 26	43	1.9218	-0.79729	0.01823	-1.0088
Bus 29	Bus 28	44	3.4909	-0.51886	0.01479	-0.13157
Bus 38	Bus 29	45	8.3	-0.02723	0.0523	1.0199
Bus 31	Bus 06	46	5.1092	2.5614	0	0.84683

GLOBAL SUMMARY REPORT

TOTAL GENERATION

REAL POWER [p.u.]	61.3092
REACTIVE POWER [p.u.]	11.6962

TOTAL LOAD

REAL POWER [p.u.]	60.889
REACTIVE POWER [p.u.]	14.043

TOTAL LOSSES

REAL POWER [p.u.]	0.4202
REACTIVE POWER [p.u.]	-2.3468

BIBLIOGRAPHY

[1] Kundur, P., *Power System Stability and Control*, McGraw-Hill, Inc., New York, 1994

[2] Padiyar, K.R., *Power System Dynamics Stability and Control*, BS Publications, Hyderabad, 2nd edition, 2008

[3] Steinmetz, C.P., "Power Control and Stability of Electric Generating Stations," *AIEE Trans.,* Vol. XXXIX, no.2, pp.1215-1287, July 1920

[4] Wikins, R., "Practical Aspects of System Stability," *AIEE Trans.*, pp. 41-50, 1926

[5] Evans, R.D., Wagner, C.F., "Further Studies of Transmission System Stability," *AIEE Trans.*, pp. 51-80, 1926

[6] Edvard. (2010). Historical Review of Power System Stability Problems. Retrieved from http://electrical-engineering-portal.com/historical-review-of-power-system-stability-problems

[7] Bergen, A.R., Vittal, V., *Power Systems Analysis*, Prentice-Hall, Inc, New Jersey, 2nd edition, 2000

[8] Magnusson, P.C., "Transient Energy Method of Calculating Stability," *AIEE Trans.*, Vol. 66, pp. 747-755, 1947

[9] Aylett, P.D., "The Energy Integral-Criterion of Transient Stability Limits of Power Systems," *Proc. IEE,* Vol. 105c, No. 8, pp. 527-536, September 1958.

[10] Milano, F., "An Open Source Power System Analysis Toolbox," *Power Engineering Society General Meeting, 2006. IEEE*, vol. no. pp.1 pp. 0-0 0

[11] Michel, A., Fouad, A., Vittal, V., "Power system transient stability using individual machine energy functions," *Circuits and Systems, IEEE Transactions on* , vol.30, no.5, pp. 266- 276, May 1983

[12] Sauer, P. W., Pai, M. A., *Power System Dynamic and Stability*, Prentice-Hall, Inc. New Jersey, 1998

[13] Fang Da-Zhong, Chung, T.S., Zhang Yao, "Corrected transient energy function and its application to transient stability margin assessment," *Advances in Power System Control, Operation and Management, 1997. APSCOM-97. Fourth International Conference on (Conf. Publ. No. 450)* , vol.1, no., pp.310-313 vol.1, 11-14 Nov 1997

[14] Da-Zhong Fang, Chung, T.S., Yao Zhang, Wennan Song, "Transient stability limit conditions analysis using a corrected transient energy function approach," *Power Systems, IEEE Transactions on* , vol.15, no.2, pp.804-810, May 2000

[15] Rahimi, F.A., Lauby, M.G., Wrubel, J.N., Lee, K.L., "Evaluation of the transient energy function method for on-line dynamic security analysis," *Power Systems, IEEE Transactions on* , vol.8, no.2, pp.497-507, May 1993

[16] A. H. El-Abiad and K. Nagappan, "Transient Stability Regions for Multi-Machine Power Systems," *IEEE Trans. Power Apparatus and Syst.,* vol. PAS-85, pp. 169-179, 1966

[17] Athay, T., Podmore, R., Virmani, S., "A Practical Method for the Direct Analysis of Transient Stability," *IEEE Transactions on Power Apparatus and Systems*, vol.PAS-98, no.2, pp.573-584, March 1979

[18] Rastgoufard, P., Yazdankhah, A., Schlueter, R.A., "Multi-machine equal area based power system transient stability measure," *IEEE Transactions on Power Systems*, vol.3, no.1, pp.188-196, Feb 1988

[19] Haque, M.H., "Equal-area criterion: an extension for multimachine power systems," *Generation, Transmission and Distribution, IEE Proceedings* , vol.141, no.3, pp.191-197, May 1994

[20] Michel, A., Fouad, A., Vittal, V., "Power system transient stability using individual machine energy functions," *IEEE Transactions on Circuits and Systems*, vol.30, no.5, pp. 266- 276, May 1983

[21] Pai, M. A., *Energy Function Analysis for Power System Stability*, Kluwer Academic Publishers, Massachusetts, 1989

[22] Milano, Federico, *Power System Analysis Toolbox: Quick Reference Manual for PSAT version 2.1.2*, June 28, 2008

[23] Hsiao-Dong Chang, Chia-Chi Chu, Cauley, G., "Direct stability analysis of electric power systems using energy functions: theory, applications, and perspective," *Proceedings of the IEEE* , vol.83, no.11, pp.1497-1529, Nov 1995

[24] Milano, F., *Power System Modeling and Scripting*, Springer-Verlag London Limited, London, 2010

[25] Vittal, V., "Extending applications of the transient energy function method," *Circuits and Systems, 1992., Proceedings of the 35th Midwest Symposium on* , vol., no., pp.1428-1431 vol.2, 9-12 Aug 1992

[26] Haque, M.H., "Application of energy function to assess the first-swing stability of a power system with a SVC," *Generation, Transmission and Distribution, IEE Proceedings-* , vol.152, no.6, pp. 806- 812, 4 Nov. 2005

[27] Lu Fang, Yu Ji-lai, "Transient stability analysis with equal area criterion directly used to a non-equivalent generator pair," *Power Engineering, Energy and Electrical Drives, 2009. POWERENG '09. International Conference on* , vol., no., pp.386-389, 18-20 March 2009

[28] Xiaoyang Wang, Yong Min, Kaiyuan Hou, "A New Method of Computing the Controlling Unstable Equilibrium Point of the Post-Fault Power System," *Power System Technology, 2006. PowerCon 2006. International Conference on* , vol., no., pp.1-5, 22-26 Oct. 2006

[29] Treinen, R.T., Vittal, V., Kliemann, W., "An improved technique to determine the controlling unstable equilibrium point in a power system," *Circuits and Systems I: Fundamental Theory and Applications, IEEE Transactions on* , vol.43, no.4, pp.313-323, Apr 1996

[30] Priyadi, A., Yorino, N., Jha, D.K., Zoka, Y., Sasaki, Y., Yasuda, H., Kakui, H., "Critical Trajectory Method for Transient Stability Analysis," *Computer and Electrical Engineering, 2008. ICCEE 2008. International Conference on* , vol., no., pp.291-295, 20-22 Dec. 2008

[31] Priyadi, A., Yorino, N., Eghbal, M., Zoka, Y., Sasaki, Y., Yasuda, H., Kakui, H., "Transient stability assessment as boundary value problem," *Electric Power Conference, 2008. EPEC 2008. IEEE Canada* , vol., no., pp.1-6, 6-7 Oct. 2008

[32] Li Zhengdao, Liu Sheng, Chen Chen, "New algorithm for the solution of controlling unstable equilibrium point," *Power System Technology, 2002. Proceedings. PowerCon 2002. International Conference on* , vol.4, no., pp. 1999- 2003 vol.4, 2002

VITA

The author was born in 1982 in the Kingdom of Saudi Arabia. He completed his associate diploma in Electrical Power Engineering Technology from Jubail Industrial College, Jubail, Saudi Arabia in 2004 with first honor degree. He finished his Bachelor of Science degree in Electrical Engineering from the University of New Orleans in December 2008 with Cum Laude honor. He is expected to finish his Masters in Electrical Engineering from the University of New Orleans in May 2011. His areas of interests are power systems stability analysis and on-line transient stability assessment.